

Optimal Sparse Principal Component Analysis in High Dimensional Elliptical Model

Fang Han* and Han Liu†

October 15, 2013

Abstract

We propose a semiparametric sparse principal component analysis method named elliptical component analysis (ECA) for analyzing high dimensional non-Gaussian data. In particular, we assume the data follow an elliptical distribution. Elliptical family contains many well-known multivariate distributions such as multivariate Gaussian, multivariate- t , Cauchy, Kotz, and logistic distributions. It allows extra flexibility on modeling heavy-tailed distributions and capture tail dependence between variables. Such modeling flexibility makes it extremely useful in modeling financial, genomics and bioimaging data, where the data typically present heavy tails and high tail dependence. Under a double asymptotic framework where both the sample size n and the dimension d increase, we show that a multivariate rank based ECA procedure attains the optimal rate of convergence in parameter estimation. This is the first optimality result established for sparse principal component analysis on high dimensional elliptical data.

Keyword: Sparse principal component analysis; Optimal rates of convergence; Double asymptotics; Robust estimators; Elliptical distribution.

1 Introduction

This paper considers sparse principal component analysis (PCA) for high dimensional non-Gaussian data. Let $\mathbf{x}_1, \dots, \mathbf{x}_n$ be n data points of a random vector $\mathbf{X} \in \mathbb{R}^d$. We denote Σ to be the covariance matrix of \mathbf{X} and $\mathbf{u}_1, \dots, \mathbf{u}_m$ to be its top m leading eigenvectors. We want to find $\hat{\mathbf{u}}_1, \dots, \hat{\mathbf{u}}_m$ that can estimate $\mathbf{u}_1, \dots, \mathbf{u}_m$ accurately.

We consider the high dimensional setting under which the dimension d increases with the sample size n with the possibility $d \gg n$. Compared with the classical asymptotic theory in

*Department of Biostatistics, Johns Hopkins University, Baltimore, MD 21205, USA; e-mail: fhan@jhsp.hopkins.edu

†Department of Operations Research and Financial Engineering, Princeton University, Princeton, NJ 08544, USA; e-mail: hanliu@princeton.edu

which d is fixed, this framework more realistically reflects the challenge of many real-world applications. We refer to Meinshausen and Bühlmann (2006), Bickel and Levina (2008), and Bühlmann and van de Geer (2011) for more thorough discussions. Under this framework, the classical PCA has been shown to be inconsistent under many conditions (Johnstone and Lu, 2009). In particular, the angle between the PCA estimator $\hat{\mathbf{u}}_1$ and \mathbf{u}_1 may not converge to 0 if $d/n \rightarrow c$ for some constant $c > 0$. To avoid this curse of dimensionality, certain types of sparsity assumptions are needed. For example, when estimating the leading eigenvector $\mathbf{u}_1 := (u_{11}, \dots, u_{1d})^T$, we may assume that \mathbf{u}_1 is sparse, i.e., $s := \text{card}(\{j : u_{1j} \neq 0\}) < n$. By exploiting this sparsity structure, different variants of sparse PCA have been proposed (d’Aspremont et al., 2007; Zou et al., 2006; Shen and Huang, 2008; Witten et al., 2009; Journée et al., 2010; Zhang and El Ghaoui, 2011). The theoretical properties of these and related methods have been analyzed under both Gaussian and sub-Gaussian assumptions (Jung and Marron, 2009; Amini and Wainwright, 2009; Shen et al., 2011; Ma, 2013; Vu and Lei, 2012, 2013; Berthet and Rigollet, 2013; Lounici, 2013; Birnbaum et al., 2013; Cai et al., 2013). In particular, Vu and Lei (2012) showed that the rate of convergence $O(\sqrt{s \log d/n})$ is minimax optimal under a certain model class.

One limitation for the existing sparse PCA theories is that they rely heavily on the Gaussian or sub-Gaussian assumption. If the Gaussian assumption is correct, accurate estimation can be expected, otherwise, the obtained result can be misleading. To relax the Gaussian assumption, Han and Liu (2013) generalized the Gaussian to the semiparametric transelliptical family (called “meta-elliptical” in their paper) for modeling the data. The transelliptical family assumes that after unspecified increasing marginal transformations, the data are elliptically distributed. By resorting to the marginal rank-based correlation coefficient estimator (e.g., Kendall’s tau), Han and Liu (2013) proposed a semiparametric scale-invariant PCA named transelliptical component analysis (TCA). A rate of convergence $O(s\sqrt{\log d/n})$ is established for estimating the leading eigenvector $\boldsymbol{\theta}_1$ of the (latent) correlation matrix without any constrain on the moments. Despite all these efforts, there are two remaining problems of their work. First, using marginal ranks, they can only conduct scale-invariant PCA, i.e., estimating the leading eigenvectors of the correlation instead of the covariance matrix. Second, it is unclear whether their obtained rate of convergence is minimax optimal or not.

In this paper we show that, under the elliptical model, the rate of convergence for the marginal rank-based estimators proposed in Han and Liu (2013) is suboptimal. Instead, we present an alternative procedure that achieves the minimax optimal rate of convergence in estimating \mathbf{u}_1 . The main idea is to exploit a multivariate version of the Kendall’s tau statistic to directly estimate the eigenvectors of $\boldsymbol{\Sigma}$ and treat the eigenvalues of $\boldsymbol{\Sigma}$ as nuisance parameters. In particular, letting $\angle(\mathbf{u}_1, \hat{\mathbf{u}}_1^*)$ be the angle between the ECA estimate $\hat{\mathbf{u}}_1^*$ and

the leading eigenvector \mathbf{u}_1 of Σ , we provide an explicit rate of convergence for $\sin \angle(\mathbf{u}_1, \widehat{\mathbf{u}}_1^*)$:

$$\mathbb{E}|\sin \angle(\mathbf{u}_1, \widehat{\mathbf{u}}_1^*)| = O\left(\sqrt{\frac{s \log d}{n}}\right),$$

which is the parametric optimal rate of convergence obtained by Vu and Lei (2012) under the (sub)Gaussian model. This result suggests that the extra modeling flexibility of ECA comes at almost no cost of statistical efficiency.

ECA is fundamentally different from TCA (Han and Liu, 2013) in three aspects: (i) ECA aims at estimating the leading eigenvector of the covariance matrix of an elliptical distribution, while TCA can only estimate the leading eigenvector of the latent correlation matrix of a transelliptical distribution; (ii) ECA can estimate the principal components, while TCA cannot due to the lack of specification of the marginal transformations; (iii) Confined in the elliptical distribution, the rate of convergence of ECA is minimax optimal and is faster than that of TCA.

The rest of this paper is organized as follows. In the next section, we briefly introduce the elliptical distribution and review the marginal rank-based estimators. In Section 3, we present the statistical model of ECA, introduce the corresponding multivariate rank-based estimators. We provide theoretical results in Section 4. In Section 5 we provide empirical studies on both synthetic and real-world data. The technical proofs are put in Section 6. More conclusions and discussions are provided in Section 7.

2 Background

In this section, we briefly review the elliptical distribution and marginal rank-based estimators. We start with an introduction of notation: Let $\mathbf{M} = [\mathbf{M}_{jk}] \in \mathbb{R}^{d \times d}$ be a symmetric matrix and $\mathbf{v} = (v_1, \dots, v_d)^T \in \mathbb{R}^d$ be a vector, we denote \mathbf{v}_I to be the subvector of \mathbf{v} whose entries are indexed by a set I , and $\mathbf{M}_{I,J}$ to be the submatrix of \mathbf{M} whose rows are indexed by I and columns are indexed by J . We denote $\text{supp}(\mathbf{v}) := \{j : v_j \neq 0\}$. For $0 < q < \infty$, we define the ℓ_q and ℓ_∞ vector norms as

$$\|\mathbf{v}\|_q := \left(\sum_{i=1}^d |v_i|^q\right)^{1/q} \text{ and } \|\mathbf{v}\|_\infty := \max_{1 \leq i \leq d} |v_i|.$$

We denote $\|\mathbf{v}\|_0 := \text{card}(\text{supp}(\mathbf{v}))$. We define the matrix ℓ_{\max} norm as the elementwise maximum value: $\|\mathbf{M}\|_{\max} := \max\{|\mathbf{M}_{ij}|\}$. Let $\Lambda_j(\mathbf{M})$ be the j -th largest eigenvalue of \mathbf{M} . In particular, $\Lambda_{\min}(\mathbf{M}) := \Lambda_d(\mathbf{M})$ and $\Lambda_{\max}(\mathbf{M}) := \Lambda_1(\mathbf{M})$ are the smallest and largest eigenvalues of \mathbf{M} . Let $\Theta_j(\mathbf{M})$ be the eigenvector of \mathbf{M} corresponding to $\Lambda_j(\mathbf{M})$. With no loss of generality, we assume that the first nonzero entry of $\Theta_j(\mathbf{M})$ is positive. We denote $\|\mathbf{M}\|_2$ to be the spectral norm of \mathbf{M} and $\mathbb{S}^{d-1} := \{\mathbf{v} \in \mathbb{R}^d : \|\mathbf{v}\|_2 = 1\}$ to be the d -dimensional unit sphere. We define the restricted spectral norm $\|\mathbf{M}\|_{2,s} := \sup_{\mathbf{v} \in \mathbb{S}^{d-1}, \|\mathbf{v}\|_0 \leq s} |\mathbf{v}^T \mathbf{M} \mathbf{v}|$. For

any matrix \mathbf{M} , we denote $f(\mathbf{M})$ to be the matrix with entries $[f(\mathbf{M})]_{jk} = f(\mathbf{M}_{jk})$. For any matrix $\mathbf{M} \in \mathbb{R}^{d \times d}$, we denote $\text{diag}(\mathbf{M})$ to be the diagonal matrix with the same diagonal entries as \mathbf{M} .

2.1 Elliptical Distribution

In this section we overview the elliptical distribution. We denote $\mathbf{X} \stackrel{d}{=} \mathbf{Y}$ if random vectors \mathbf{X} and \mathbf{Y} have the same distribution. Following the discussion in Fang et al. (1990), the elliptical distribution is defined as follows.

Definition 2.1 (Elliptical distribution). *Let $\boldsymbol{\mu} \in \mathbb{R}^d$ and $\boldsymbol{\Sigma} \in \mathbb{R}^{d \times d}$ with $\text{rank}(\boldsymbol{\Sigma}) = q \leq d$. A d -dimensional random vector \mathbf{X} has an elliptical distribution, denoted by $\mathbf{X} \sim EC_d(\boldsymbol{\mu}, \boldsymbol{\Sigma}, \xi)$, if it has a stochastic representation*

$$\mathbf{X} \stackrel{d}{=} \boldsymbol{\mu} + \xi \mathbf{A} \mathbf{U}, \quad (2.1)$$

where \mathbf{U} is a uniform random vector on the unit sphere in \mathbb{R}^q , $\xi \geq 0$ is a scalar random variable independent of \mathbf{U} , $\mathbf{A} \in \mathbb{R}^{d \times q}$ is a deterministic matrix satisfying $\mathbf{A} \mathbf{A}^T = \boldsymbol{\Sigma}$. Here $\boldsymbol{\Sigma}$ is called the scatter matrix.

An equivalent definition of the elliptical distribution is that its characteristic function can be written as $\exp(i\mathbf{t}^T \boldsymbol{\mu}) \psi(\mathbf{t}^T \boldsymbol{\Sigma} \mathbf{t})$, where ψ is a properly defined characteristic function and $i := \sqrt{-1}$. ξ and ψ are uniquely determined by one of the other. In this setting, we denote by $\mathbf{X} \sim EC_d(\boldsymbol{\mu}, \boldsymbol{\Sigma}, \psi)$. Moreover, we have the following proposition, which states that whenever $\mathbb{E}\xi^2$ exists, the eigenvectors of the scatter matrix $\boldsymbol{\Sigma}$ is the same as the eigenvectors of $\text{Cov}(\mathbf{X})$.

Proposition 2.2 (Fang et al. (1990)). *When $\mathbf{X} \sim EC_d(\boldsymbol{\mu}, \boldsymbol{\Sigma}, \xi)$, $\mathbb{E}\mathbf{X} = \boldsymbol{\mu}$ and when $\mathbb{E}\xi^2$ exists, $\text{Cov}(\mathbf{X}) = \frac{\mathbb{E}\xi^2}{q} \boldsymbol{\Sigma}$. Moreover, when $\mathbb{E}\xi^2$ exists, if $\Lambda_j(\boldsymbol{\Sigma}) \neq \Lambda_k(\boldsymbol{\Sigma})$ for any $k \neq j$, we have*

$$\mathbf{u}_j := \boldsymbol{\Theta}_j(\boldsymbol{\Sigma}) = \boldsymbol{\Theta}_j(\text{Cov}(\mathbf{X})). \quad (2.2)$$

The model in Definition 2.1 is not identifiable. For example, when $\mathbf{X} \sim EC_d(\boldsymbol{\mu}, \boldsymbol{\Sigma}, \xi)$, for any positive constant c and matrix $\mathbf{A} \in \mathbb{R}^{d \times q}$ such that $\mathbf{A} \mathbf{A}^T = \boldsymbol{\Sigma}$, we also have $\mathbf{X} \stackrel{d}{=} \boldsymbol{\mu} + \xi \mathbf{A} \mathbf{U} \stackrel{d}{=} \boldsymbol{\mu} + (\xi/c)(c\mathbf{A})\mathbf{U}$. Therefore, the matrix $\boldsymbol{\Sigma}$ is unique only up to a constant scaling. To make the model identifiable, we assume that the maximum of the diagonals of $\boldsymbol{\Sigma}$ to be 1. For continuous elliptical distribution, $\boldsymbol{\Sigma}_{jj} > 0$ for $j = 1, \dots, d$. We define the *generalized correlation matrix* $\boldsymbol{\Sigma}^0$ to be $\boldsymbol{\Sigma}^0 := \text{diag}(\boldsymbol{\Sigma})^{-1/2} \cdot \boldsymbol{\Sigma} \cdot \text{diag}(\boldsymbol{\Sigma})^{-1/2}$. It is easy to see that $\boldsymbol{\Sigma}^0$ is the correlation matrix of \mathbf{X} whenever $\mathbb{E}\xi^2$ exists.

Compared to the Gaussian family, the elliptical family is much more flexible in modeling complex data. First, elliptical family can model heavy-tail distributions (In contrast,

Gaussian is light-tailed and the extreme event must go to zero exponentially fast). Secondly, elliptical family can be used to model nontrivial tail dependence between variables (Hult and Lindskog, 2002), i.e., different variables tend to go to extremes together (In contrast, Gaussian family can not capture any tail distributions). The capability to handle heavy-tailed distributions and tail dependence are extremely important for machine learning methods to be applied to analyze real-world data from a wide range of areas, including (1) Financial data (almost all the financial data have heavy-tailed and tail dependence issues, see, for example, Rachev (2003) and Pavel et al. (2005)); (2) Genomics data (Liu et al. (2003) and Posekany et al. (2011) showed that many microarray data are heavy-tailed even after normalization); (3) Bioimaging data (fMRI data have heavy tails, see, for example, Ruttimann et al. (1998)).

2.2 The Marginal Rank-based Estimators

In this section we briefly review the marginal rank-based estimator which uses the marginal Kendall's tau statistic. This statistic plays a vital role for estimating the leading eigenvectors of the generalized correlation matrix Σ^0 in Han and Liu (2013). Letting $\mathbf{X} := (X_1, \dots, X_d)^T \in \mathbb{R}^d$ and $\tilde{\mathbf{X}} := (\tilde{X}_1, \dots, \tilde{X}_d)^T$ be an independent copy of \mathbf{X} , the population version of the Kendall's tau statistic is defined as:

$$\tau(X_j, X_k) := \text{Corr}(\text{sign}(X_j - \tilde{X}_j), \text{sign}(X_k - \tilde{X}_k)).$$

Let $\mathbf{x}_1, \dots, \mathbf{x}_n \in \mathbb{R}^d$ with $\mathbf{x}_i := (x_{i1}, \dots, x_{id})^T$ be n independent observations of \mathbf{X} . The sample version marginal Kendall's tau statistic is defined as:

$$\hat{\tau}_{jk}(\mathbf{x}_1, \dots, \mathbf{x}_n) := \frac{2}{n(n-1)} \sum_{1 \leq i < i' < n} \text{sign}(x_{ij} - x_{i'j}) \text{sign}(x_{ik} - x_{i'k}).$$

It is easy to verify that $\mathbb{E} \hat{\tau}_{jk}(\mathbf{x}_1, \dots, \mathbf{x}_n) = \tau(X_j, X_k)$. Let $\hat{\mathbf{R}} = [\hat{\mathbf{R}}_{jk}] \in \mathbb{R}^{d \times d}$ with $\hat{\mathbf{R}}_{jk} = \sin(\frac{\pi}{2} \hat{\tau}_{jk}(\mathbf{x}_1, \dots, \mathbf{x}_n))$ be the Kendall's tau correlation matrix. The marginal rank-based estimator $\hat{\boldsymbol{\theta}}_1$ used by TCA is obtained by plugging $\hat{\mathbf{R}}$ into the optimization formulation in Vu and Lei (2012). When $\mathbf{X} \sim EC_d(\boldsymbol{\mu}, \boldsymbol{\Sigma}, \xi)$ and with certain conditions, Han and Liu (2013) showed that

$$\mathbb{E} |\sin \angle(\tilde{\boldsymbol{\theta}}_1, \boldsymbol{\Theta}_1(\boldsymbol{\Sigma}^0))| = O\left(s \sqrt{\frac{\log d}{n}}\right),$$

where $s := \|\boldsymbol{\Theta}_1(\boldsymbol{\Sigma}^0)\|_0$ and $\boldsymbol{\Sigma}^0$ is the generalized correlation matrix of \mathbf{X} . However, TCA can be viewed as a variant of the scale-invariant PCA and can only estimate the leading eigenvector of the correlation matrix. Then how to estimate the leading eigenvector of the covariance matrix in high dimensional elliptical models? A straightforward approach is to exploit a covariance matrix estimator $\hat{\mathbf{S}} := [\hat{\mathbf{S}}_{jk}]$ defined as

$$\hat{\mathbf{S}}_{jk} = \hat{\mathbf{R}}_{jk} \cdot \hat{\sigma}_j \hat{\sigma}_k, \tag{2.3}$$

where $\{\widehat{\sigma}_j\}_{j=1}^d$ are sample standard deviations. However, since the elliptical distribution can be heavy-tailed, estimating the standard deviations is challenging and makes the corresponding estimator less efficient. In this paper, we solve this problem by resorting to the multivariate rank-based method.

3 Elliptical Component Analysis

In this paper, we propose a multivariate rank-based multivariate rank-based approach for estimating the leading eigenvector \mathbf{u}_1 of Σ under an elliptical model.

3.1 Multivariate Rank-based Estimators

We first provide the definition and several basic properties of multivariate rank-based estimators. Our main idea is based on the multivariate Kendall's tau statistic, which is first introduced in Choi and Marden (1998) for testing independence and is further used in estimating low-dimensional covariance matrices (Visuri et al., 2000; Oja, 2010) and principal components (Marden, 1999; Croux et al., 2002; Jackson and Chen, 2004). Some related methods using multivariate rank-based statistics have also been discussed in Tyler (1982), Tyler (1987), Taskinen et al. (2003), Oja and Randles (2004), Oja and Paindaveine (2005), Oja et al. (2006), and Sirkiä et al. (2007). Their theoretical performance in low dimensions were analyzed in Hallin and Paindaveine (2002b,a, 2004, 2005, 2006) and Hallin et al. (2006).

Though significant progress has been made, the current theoretical results are mainly on low dimensional settings in which $d < n$. To the best of our knowledge, there is no result on generalizing this statistic to the high dimensional settings. In this paper, we will propose ECA based on the multivariate Kendall's tau statistic. In high dimensions, we first time show that ECA is minimax optimal in estimating the leading eigenvector \mathbf{u}_1 .

More specifically, the population and empirical versions of the multivariate Kendall's tau are defined as follows. Let $\mathbf{X} \sim EC_d(\boldsymbol{\mu}, \Sigma, \xi)$ and $\widetilde{\mathbf{X}}$ be an independent copy of \mathbf{X} . The population multivariate Kendall's tau matrix, denoted by $\mathbf{K} \in \mathbb{R}^{d \times d}$, is defined as:

$$\mathbf{K} := \mathbb{E} \left(\frac{(\mathbf{X} - \widetilde{\mathbf{X}})(\mathbf{X} - \widetilde{\mathbf{X}})^T}{\|\mathbf{X} - \widetilde{\mathbf{X}}\|_2^2} \right). \quad (3.1)$$

Let $\mathbf{x}_1, \dots, \mathbf{x}_n$ be n independent data points of a random vector $\mathbf{X} \sim EC_d(\boldsymbol{\mu}, \Sigma, \xi)$. By the previous discussion, we define the sample version multivariate Kendall's tau estimator as

$$\widehat{\mathbf{K}} = \frac{1}{n(n-1)} \sum_{i \neq j} \frac{(\mathbf{x}_i - \mathbf{x}_j)(\mathbf{x}_i - \mathbf{x}_j)^T}{\|\mathbf{x}_i - \mathbf{x}_j\|_2^2}.$$

It is easy to verify that $\mathbb{E}(\widehat{\mathbf{K}}) = \mathbf{K}$. Moreover, each entry in \mathbf{K} and $\widehat{\mathbf{K}}$ is upper bounded by 1 and lower bounded by -1 . Such boundedness makes $\widehat{\mathbf{K}}$ more amenable to theoretical analysis.

We then have the following proposition, which states that the eigenvectors of the multivariate Kendall's tau statistic \mathbf{K} are identical to the eigenvectors of $\boldsymbol{\Sigma}$. This proposition is stated in Oja (2010) and will play a key role in constructing the ECA procedure.

Proposition 3.1 (Oja (2010)). *Let $\mathbf{X} \sim EC_d(\boldsymbol{\mu}, \boldsymbol{\Sigma}, \xi)$ be a continuous distribution and \mathbf{K} be the population multivariate Kendall's tau statistic. Then if $\Lambda_j(\boldsymbol{\Sigma}) \neq \Lambda_k(\boldsymbol{\Sigma})$ for any $k \neq j$, we have*

$$\boldsymbol{\Theta}_j(\boldsymbol{\Sigma}) = \boldsymbol{\Theta}_j(\mathbf{K}) \quad \text{and} \quad \Lambda_j(\mathbf{K}) = \mathbb{E} \left(\frac{\Lambda_j(\boldsymbol{\Sigma})U_j^2}{\Lambda_1(\boldsymbol{\Sigma})U_1^2 + \dots + \Lambda_d(\boldsymbol{\Sigma})U_d^2} \right), \quad (3.2)$$

where $\mathbf{U} := (U_1, \dots, U_d)^T$ follows a uniform distribution on \mathbb{S}^{d-1} . In particular, when $\mathbb{E}\xi^2$ exists, we have $\boldsymbol{\Theta}_j(\text{Cov}(\mathbf{X})) = \boldsymbol{\Theta}_j(\mathbf{K})$.

Remark 3.2. *Proposition 3.1 states that the multivariate Kendall's tau statistic is invariant to the generating variable ξ in estimating leading eigenvectors of the covariance matrix $\boldsymbol{\Sigma}$. Therefore, this estimator is invariant within the whole elliptical family.*

3.2 ECA Model and Method

In this section we provide the model and method of elliptical component analysis (ECA). ECA aims at recovering the leading eigenvector of the covariance matrix (when it exists) in a high dimensional elliptical model. In particular, the following model $\mathcal{M}_d(\boldsymbol{\Sigma}, \xi, s; \kappa_L, \kappa_U)$ is considered:

$$\mathcal{M}_d(\boldsymbol{\Sigma}, \xi, s; \kappa_L, \kappa_U) : \begin{cases} \mathbf{X} \sim EC_d(\boldsymbol{\mu}, \boldsymbol{\Sigma}, \xi), \\ \|\boldsymbol{\Theta}_1(\boldsymbol{\Sigma})\|_0 \leq s, \Lambda_1(\boldsymbol{\Sigma}) \geq \kappa_L \Lambda_2(\boldsymbol{\Sigma}), \Lambda_1(\boldsymbol{\Sigma}) \leq \kappa_U \Lambda_d(\boldsymbol{\Sigma}), \\ \text{and } \mathbb{P}(\xi = 0) = 0. \end{cases} \quad (3.3)$$

Here $\kappa_L, \kappa_U > 1$ are two absolute constants.

Given the model $\mathcal{M}_d(\boldsymbol{\Sigma}, \xi, s; \kappa_L, \kappa_U)$ and inspired by Proposition 3.1, we can plug $\widehat{\mathbf{K}}$ into any sparse PCA algorithm for conducting ECA. The most intuitive ECA estimator is the optimum to the following optimization problem to estimate $\mathbf{u}_1 := \boldsymbol{\Theta}_1(\boldsymbol{\Sigma})$:

$$\begin{aligned} \widehat{\mathbf{u}}_1^* &= \arg \max_{\mathbf{v} \in \mathbb{R}^d} \mathbf{v}^T \widehat{\mathbf{K}} \mathbf{v}, \\ &\text{subject to } \mathbf{v} \in \mathbb{S}^{d-1} \cap \mathbb{B}_0(s), \end{aligned} \quad (3.4)$$

where $\mathbb{B}_0(s) := \{\mathbf{v} \in \mathbb{R}^d : \|\mathbf{v}\|_0 \leq s\}$ and $\widehat{\mathbf{K}}$ is the estimated multivariate Kendall's tau matrix. The corresponding global optimum is denoted by $\widehat{\mathbf{u}}_1^*$. Using Proposition 2.2, $\widehat{\mathbf{u}}_1^*$ is also an estimator of $\boldsymbol{\Theta}_1(\text{Cov}(\mathbf{X}))$, whenever the covariance matrix exists.

Moreover, we would like to note that, although the optimization in (3.4) is essentially combinatoric and hard to compute, this formulation provides theoretical insights on the properties of ECA. In practice, we can exploit many methods to approximately calculate this global estimator. Examples include the methods proposed in Jolliffe et al. (2003), d’Aspremont et al. (2007), Zou et al. (2006), Shen and Huang (2008), Witten et al. (2009), and Yuan and Zhang (2013).

To illustrate this problem more clearly, we consider one computationally tractable ECA algorithm by plugging $d\widehat{\mathbf{K}}$ into the truncated power method proposed in Yuan and Zhang (2013). For any matrix $\mathbf{M} \in \mathbb{R}^{d \times d}$ as an input, the truncated power method calculates a sparse vector as the loading vector estimator via exploiting a modified version of the power method. We will show in Section 4 that, using a similar technique as in the analysis of $\widehat{\mathbf{u}}_1^*$, the ECA estimator $\tilde{\mathbf{u}}_1$ by using the truncated power method can attain the same rate of convergence as $\widehat{\mathbf{u}}_1^*$. We would also like to note that, by resorting to the deflation method shown in Mackey (2009), ECA can also efficiently estimate the top m leading eigenvectors. The detailed algorithm of ECA for estimating the top one and top m leading eigenvectors using the truncated power method is provided in Appendix A.

4 Theoretical Properties

In this section, the theoretical properties of the ECA estimator are provided. In the analysis we allow the dimensional d to increase with the sample size n , with possibly $d \gg n$. This framework better reflects the challenges of many real-world applications. For example, on modeling the microarray data, we obtain the expression levels of d genes for n samples. In a typical setting, n could be hundreds while d could be tens of thousands.

Our main results state that under the elliptical model, the estimator $\widehat{\mathbf{u}}_1^*$ obtained by Equation (3.4) can approximate $\mathbf{u}_1 := \Theta_1(\boldsymbol{\Sigma})$ in the parametric optimal rate of convergence with respect to (n, d, s) .

In the sequel, we say that the model $\mathcal{M}_d(\boldsymbol{\Sigma}, \xi, s; \kappa_L, \kappa_U)$ holds if the data points $\mathbf{x}_1, \dots, \mathbf{x}_n$ are drawn from a random vector $\mathbf{X} \in \mathcal{M}_d(\boldsymbol{\Sigma}, \xi, s; \kappa_L, \kappa_U)$.

Theorem 4.1 (Parameter Estimation). *Let $\widehat{\mathbf{u}}_1^*$ be the global optimum to Equation (3.4) and the model $\mathcal{M}_d(\boldsymbol{\Sigma}, \xi, s; \kappa_L, \kappa_U)$ hold. For any two vectors $\mathbf{v}_1 \in \mathbb{S}^{d-1}$ and $\mathbf{v}_2 \in \mathbb{S}^{d-1}$, we define*

$$|\sin \angle(\mathbf{v}_1, \mathbf{v}_2)| := \sqrt{1 - (\mathbf{v}_1^T \mathbf{v}_2)^2}.$$

Then there exists a constant K only depending on κ_L and κ_U , such that for all $d \geq 3$, with probability no smaller than $1 - 2\alpha$,

$$|\sin \angle(\widehat{\mathbf{u}}_1^*, \mathbf{u}_1)| \leq K \sqrt{\frac{2s(3 + \log(d/2s)) + \log(1/\alpha)}{n}}.$$

Our main proof of Theorem 4.1 is presented in Section 6. When $\mathbb{E}\xi^2$ exists, we have $\text{Cov}(\mathbf{X})$ exists and by Proposition 2.2, \mathbf{u}_1 is also the leading eigenvector of $\text{Cov}(\mathbf{X})$. Combined with Theorem 2.2 in Vu and Lei (2012), Theorem 4.1 shows that ECA attains the parametric rate of convergence, which is $O_P(\sqrt{s \log d/n})$. Given Theorem 4.1, we immediately get the following corollary, which quantifies the expected angle between $\hat{\mathbf{u}}_1^*$ and \mathbf{u}_1 .

Corollary 4.2. *If the conditions in Theorem 4.1 hold, we have*

$$\mathbb{E} \sin^2 \angle(\hat{\mathbf{u}}_1^*, \mathbf{u}_1) \leq K^2 \cdot \frac{2s(3 + \log(d/2s)) + \log n}{n} + \frac{2}{n}.$$

Corollary 4.2 provides an upper bound on the expected difference between $\hat{\mathbf{u}}_1^*$ and \mathbf{u}_1 under the elliptical model. This result, combined with the lower bound presented in Theorem 2.1 of Vu and Lei (2012) and the fact that the elliptical distribution family is strictly larger than the Gaussian distribution family, shows that ECA is minimax optimal.

In the next corollary, we provide a feature selection consistency result for $\hat{\mathbf{u}}_1^*$. Corollary 4.3 shows that the entries in \mathbf{u}_1 that are nonzero can be recovered under the condition that the minimum absolute value of the signal part of \mathbf{u}_1 does not decay to zero too fast. Moreover, if we know the exact number of nonzero entries in \mathbf{u}_1 , then the sparsity pattern of \mathbf{u}_1 can be recovered with high probability.

Corollary 4.3 (Feature Selection). *If the conditions in Theorem 4.1 hold, let*

$$\Upsilon := \text{supp}(\mathbf{u}_1) \quad \text{and} \quad \hat{\Upsilon} := \text{supp}(\hat{\mathbf{u}}_1^*).$$

If we further have

$$\min_{j \in \Upsilon} |u_{1j}| \geq \sqrt{2}K \cdot \sqrt{\frac{2s(3 + \log(d/2s)) + \log(1/\alpha)}{n}},$$

then

$$\mathbb{P}(\Upsilon \subset \hat{\Upsilon}) \geq 1 - 2\alpha.$$

Moreover, if $\|\Theta_1(\Sigma)\|_0 = s$, then

$$\mathbb{P}(\Upsilon = \hat{\Upsilon}) \geq 1 - 2\alpha.$$

As marked at the end of Section 3.2, although the formulation in Equation (3.4) is computationally intractable, it provides deeper insights and understanding for many sparse PCA algorithms. For example, in the following we show that, using a similar proof technique as used in the proof of Theorem 4.1, a computationally tractable algorithm, called truncated power method (Yuan and Zhang, 2013), produces an efficient estimator $\tilde{\mathbf{u}}_1$ that attains the same rate of convergence as the global optimum $\hat{\mathbf{u}}_1^*$ under appropriate conditions.

Theorem 4.4. *Let $\tilde{\mathbf{u}}_1$ be the estimator via plugging $d\widehat{\mathbf{K}}$ into Algorithm 1 in Yuan and Zhang (2013). Then when the conditions in Theorem 4.1 and the conditions in Theorem 4 in Yuan and Zhang (2013) hold for $d\mathbf{K}$, we have*

$$|\sin \angle(\tilde{\mathbf{u}}_1, \mathbf{u}_1)| = O_P\left(\sqrt{\frac{s \log d}{n}}\right).$$

Here we use $d\mathbf{K}$ instead of \mathbf{K} as the input matrix to the truncated power method. This is because $\|d\widehat{\mathbf{K}} - d\mathbf{K}\|_{2,s} = O_P(\sqrt{s \log d/n})$ and the eigenvalues of $d\mathbf{K}$ are comparable to the eigenvalues of $\mathbf{\Sigma}$, while instead $\|\widehat{\mathbf{K}} - \mathbf{K}\|_{2,s} = O_P(d^{-1}\sqrt{s \log d/n})$ and \mathbf{K} 's eigenvalues are d times smaller than the eigenvalues of $\mathbf{\Sigma}$. Similar to what we have shown in Corollary 4.3, $\tilde{\mathbf{u}}_1$ can recover the sparsity pattern of \mathbf{u}_1 with high probability under appropriate conditions.

5 Numerical Experiments

In this section we conduct study on both synthetic and real-world data to investigate the empirical performance of ECA. We use the truncated power algorithm proposed in Yuan and Zhang (2013) to approximate the global optimums $\widehat{\mathbf{u}}_j^*$ to Equation (3.4). To estimate more than one loading vectors, we exploit the deflation method proposed in Mackey (2009). Here the cardinalities of the support sets of the leading eigenvectors are treated as tuning parameters. The following three methods are considered:

- TP: the classical sparse PCA method by using the Pearson's sample covariance matrix the sufficient statistic;
- TCA: Transelliptical component analysis by using the transformed Kendall's tau covariance matrix shown in Equation (2.3) as sufficient statistic;
- ECA: Elliptical component analysis by using the multivariate kendall's tau matrix as sufficient statistic.

5.1 Simulation Study

In this section, we conduct simulation study to back up the theoretical results and further investigate the empirical performance of ECA.

5.1.1 Dependence on Sample Size and Dimension

We first illustrate the dependence of the estimation accuracy of the ECA estimator on the triplet (n, d, s) . We adopt the data generating schemes of Yuan and Zhang (2013) and

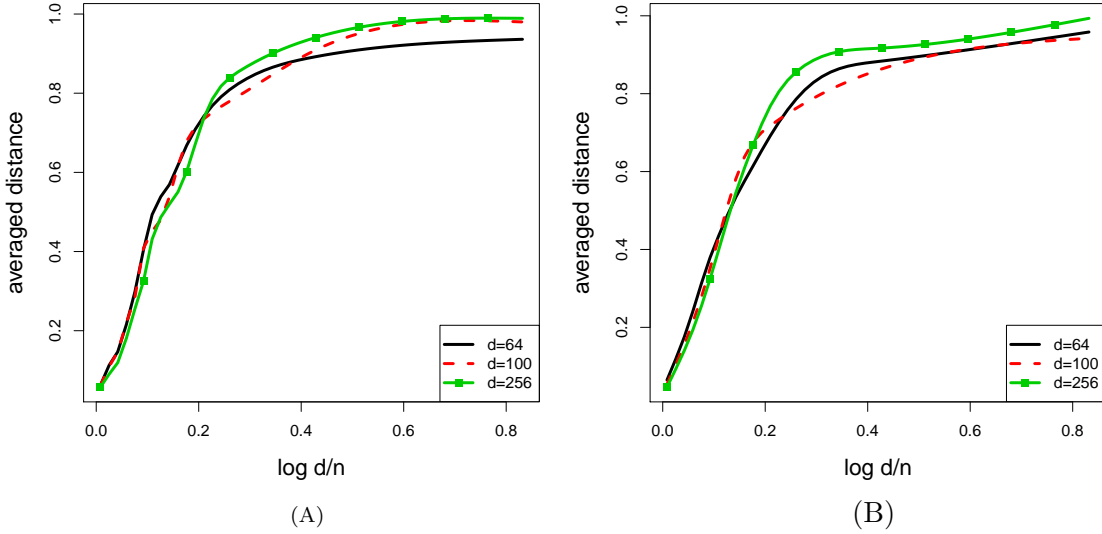


Figure 1: Simulation for two different distributions (normal and multivariate- t) with varying number of dimension d and sample size n . Plots of averaged distances between the estimators and the true parameters are conducted over 1,000 replications. (A) Normal distribution; (B) Multivariate- t distribution.

Han and Liu (2013). More specifically, we first create a scatter matrix Σ whose first two eigenvectors $\mathbf{u}_j := (u_{j1}, \dots, u_{jd})^T$ are specified to be sparse:

$$u_{1j} = \begin{cases} \frac{1}{\sqrt{10}} & 1 \leq j \leq 10 \\ 0 & \text{otherwise} \end{cases} \quad \text{and} \quad u_{2j} = \begin{cases} \frac{1}{\sqrt{10}} & 11 \leq j \leq 20 \\ 0 & \text{otherwise} \end{cases}.$$

Then we let Σ be $\Sigma = 5\mathbf{u}_1\mathbf{u}_1^T + 2\mathbf{u}_2\mathbf{u}_2^T + \mathbf{I}_d$, where $\mathbf{I}_d \in \mathbb{R}^{d \times d}$ is the identity matrix. We have $\Lambda_1(\Sigma) = 6$, $\Lambda_2(\Sigma) = 3$, $\Lambda_3(\Sigma) = \dots = \Lambda_d(\Sigma) = 1$. Using Σ as the scatter matrix, we generate n data points from a normal distribution or a multivariate- t distribution with degree of freedom 3. Here the dimension d varies from 64 to 256 and the sample size n varies from 10 to 500. Figure 1 plots the averaged angle distances $|\sin \angle(\tilde{\mathbf{u}}_1, \mathbf{u}_1)|$ between the ECA estimate $\tilde{\mathbf{u}}_1$ and the true parameter \mathbf{u}_1 , for dimensionalities $d = 64, 100, 256$, over 1,000 replications. In each setting, $s := \|\mathbf{u}_1\|_0$ is fixed to be a constant $s = 10$.

By examining the two curves in Figure 1 (A) and (B), the averaged distance between \mathbf{u}_1 and $\tilde{\mathbf{u}}_1$ starts at almost zero (for sample size n large enough), and then transits to almost one as the sample size decreases (In another word, $1/n$ increases simultaneously). Figure 1 reports that all curves almost overlapped with each other when the averaged distances are plotted against $\log d/n$. This phenomenon confirms the results in Theorems 4.1 and 4.4. Consequently, the ratio $n/\log d$ acts as an effective sample size in controlling the prediction accuracy of the eigenvectors.

Table 1: Simulation schemes with different n, d and Σ . Here the eigenvalues of Σ are set to be $\omega_1 > \dots > \omega_m > \omega_d = \dots = \omega_d$ and the top m leading eigenvectors $\mathbf{u}_1, \dots, \mathbf{u}_m$ of Σ are specified to be sparse with $s_j := \|\mathbf{u}_j\|_0$ and $u_{jk} = 1/\sqrt{s_j}$ for $k \in [1 + \sum_{i=1}^{j-1} s_i, \sum_{i=1}^j s_i]$ and zero for all the others. Σ is generated as $\Sigma = \sum_{j=1}^m (\omega_j - \omega_d) \mathbf{u}_j \mathbf{u}_j^T + \omega_d \mathbf{I}_d$. The column ‘‘Cardinalities’’ shows the cardinality of the support set of $\{\mathbf{u}_j\}$ in the form: ‘‘ $s_1, s_2, \dots, s_m, *, *, \dots$ ’’. The column ‘‘Eigenvalues’’ shows the eigenvalues of Σ in the form: ‘‘ $\omega_1, \omega_2, \dots, \omega_m, \omega_d, \omega_d, \dots$ ’’. In the first three schemes, m is set to be 2; In the second three schemes, m is set to be 4.

Scheme	n	d	Cardinalities	Eigenvalues
Scheme 1	50	100	10, 10, *, *, ...	6, 3, 1, 1, ...
Scheme 2	100	100	10, 10, *, *, ...	6, 3, 1, 1, ...
Scheme 3	100	200	10, 10, *, *, ...	6, 3, 1, 1, ...
Scheme 4	50	100	10, 8, 6, 5, *, *, ...	8, 4, 2, 1, 0.01, 0.01, ...
Scheme 5	100	100	10, 8, 6, 5, *, *, ...	8, 4, 2, 1, 0.01, 0.01, ...
Scheme 6	100	200	10, 8, 6, 5, *, *, ...	8, 4, 2, 1, 0.01, 0.01, ...

5.1.2 Estimating the Leading Eigenvector of the Scatter Matrix

To illustrate the empirical usefulness of ECA, we first focus on estimating the leading eigenvector of the scatter matrix Σ . The first three rows in Table 1 list the simulation schemes of (n, d) and Σ . In detail, let $\omega_1 > \omega_2 > \omega_d = \dots = \omega_d$ be the eigenvalues and $\mathbf{u}_1, \dots, \mathbf{u}_d$ be the eigenvectors of Σ with $\mathbf{u}_j := (u_{j1}, \dots, u_{jd})^T$. The top m leading eigenvectors $\mathbf{u}_1, \dots, \mathbf{u}_m$ of Σ are specified to be sparse such that $s_j := \|\mathbf{u}_j\|_0$ is small and

$$u_{jk} = \begin{cases} 1/\sqrt{s_j}, & 1 + \sum_{i=1}^{j-1} s_i \leq k \leq \sum_{i=1}^j s_i, \\ 0, & \text{otherwise.} \end{cases}$$

Accordingly, Σ is generated as

$$\Sigma = \sum_{j=1}^m (\omega_j - \omega_d) \mathbf{u}_j \mathbf{u}_j^T + \omega_d \mathbf{I}_d.$$

Table 1 shows the cardinalities s_1, \dots, s_m and eigenvalues $\omega_1, \dots, \omega_m$ and ω_d . In this section we consider $m = 2$.

We consider the following four different elliptical distributions:

(Normal) $\mathbf{X} \sim EC_d(\mathbf{0}, \Sigma, \xi_1)$ with $\xi_1 \stackrel{d}{=} \chi_d$. Here χ_d is the chi-distribution with degree of freedom d . For $Y_1, \dots, Y_d \stackrel{i.i.d.}{\sim} N(0, 1)$,

$$\sqrt{Y_1^2 + \dots + Y_d^2} \stackrel{d}{=} \chi_d.$$

In this setting, \mathbf{X} follows the Gaussian distribution (Fang et al., 1990).

(Multivariate- t) $\mathbf{X} \sim EC_d(\mathbf{0}, \mathbf{\Sigma}, \xi_2)$ with $\xi_2 \stackrel{d}{=} \sqrt{\kappa} \xi_1^* / \xi_2^*$. Here $\xi_1^* \stackrel{d}{=} \chi_d$ and $\xi_2^* \stackrel{d}{=} \chi_\kappa$ with $\kappa \in \mathbb{Z}^+$. In this setting, \mathbf{X} follows a multivariate- t distribution with degree of freedom κ (Fang et al., 1990). Here we consider $\kappa = 3$.

(EC1) $\mathbf{X} \sim EC_d(\mathbf{0}, \mathbf{\Sigma}, \xi_3)$ with $\xi_3 \sim F(d, 1)$, i.e., ξ_3 follows an F -distribution with degree of freedom d and 1.

(EC2) $\mathbf{X} \sim EC_d(\mathbf{0}, \mathbf{\Sigma}, \xi_4)$ with $\xi_4 \sim \text{Exp}(1)$, i.e., ξ_4 follows an exponential distribution with the rate parameter 1.

We repeatedly generate n data points according to the schemes 1 to 3 and the four distributions discussed above for 1,000 times. To show the estimation accuracy, Figure 2 plots the averaged distances between the estimate $\hat{\mathbf{u}}_1$ and true parameter \mathbf{u}_1 , defined as $|\sin \angle(\hat{\mathbf{u}}_1, \mathbf{u}_1)|$, against the numbers of estimated nonzero entries (defined as $\|\hat{\mathbf{u}}_1\|_0$), for three different methods: TP, TCA, and ECA.

To show the feature selection results for estimating the support set of the leading eigenvector \mathbf{u}_1 , Figure 3 plots the false positive rates against the true positive rates for the three different estimators under different schemes of (n, d) , $\mathbf{\Sigma}$ and different distributions.

Figure 2 shows that when the data are non-Gaussian but follow an elliptically distribution, ECA outperforms TCA and TP constantly in terms of estimation accuracy. Moreover, when the data are indeed normally distributed, there is no obvious difference between ECA and TP, indicating that ECA is a safe alternative to the classical sparse PCA under the elliptical model. Furthermore, Figure 3 verifies that, in term of feature selection, the same conclusion can be drawn.

To further strengthen the result, we conduct a quantitative comparison of the estimation accuracy of TP, TCA, and ECA. For all three methods, we fix the tuning parameter (i.e., the cardinality of the estimate's support set) to be 10. Table 2 shows the averaged distances between \mathbf{u}_1 and $\hat{\mathbf{u}}_1$, with standard deviations presented in the parentheses.

From Table 2, we see that

- (i) The estimation accuracy of the ECA estimator is significantly higher than that of TCA and TP when the data are elliptically distributed and heavy-tailed.
- (ii) There is no significant difference between ECA and TP when the data are indeed Gaussian distributed.

5.1.3 Estimating the Top m Leading Eigenvectors of the Scatter Matrix

Next, we focus on estimating the top m leading eigenvectors of the scatter matrix $\mathbf{\Sigma}$. We generate $\mathbf{\Sigma}$ in a similar way as in Section 5.1.2. We adopt the schemes 4 to 6 in Table 1 and the four distributions discussed in Section 5.1.2. We consider the case $m = 4$. We use the iterative deflation method and exploit the truncated power method in each step

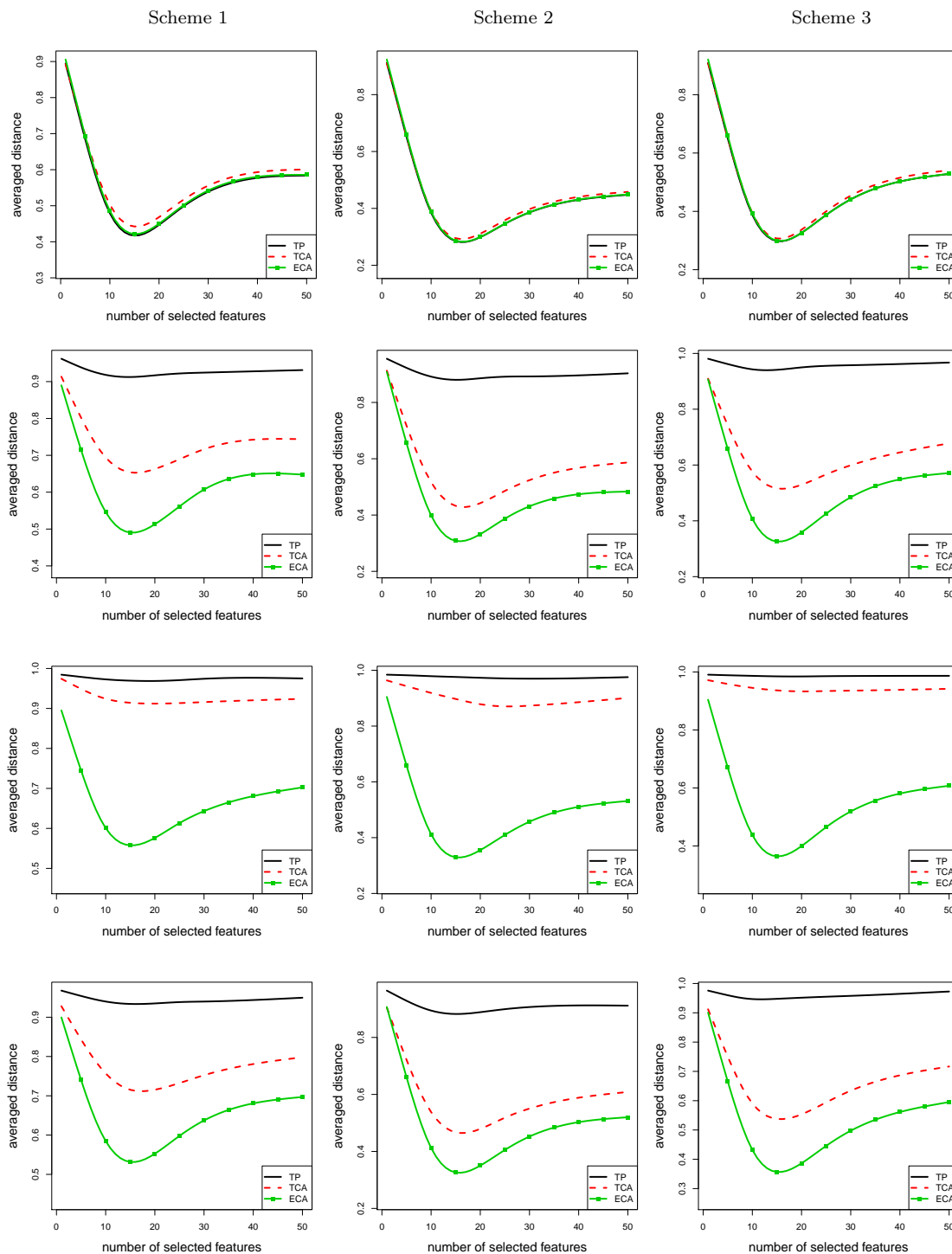


Figure 2: Curves of averaged distances between the estimates and true parameters for different schemes and distributions (normal, multivariate- t , EC1, and EC2, from top to bottom) using the truncated power method. Here we are interested in estimating the leading eigenvector. The horizontal-axis represents the cardinalities of the estimates' support sets and the vertical-axis represents the averaged distances.

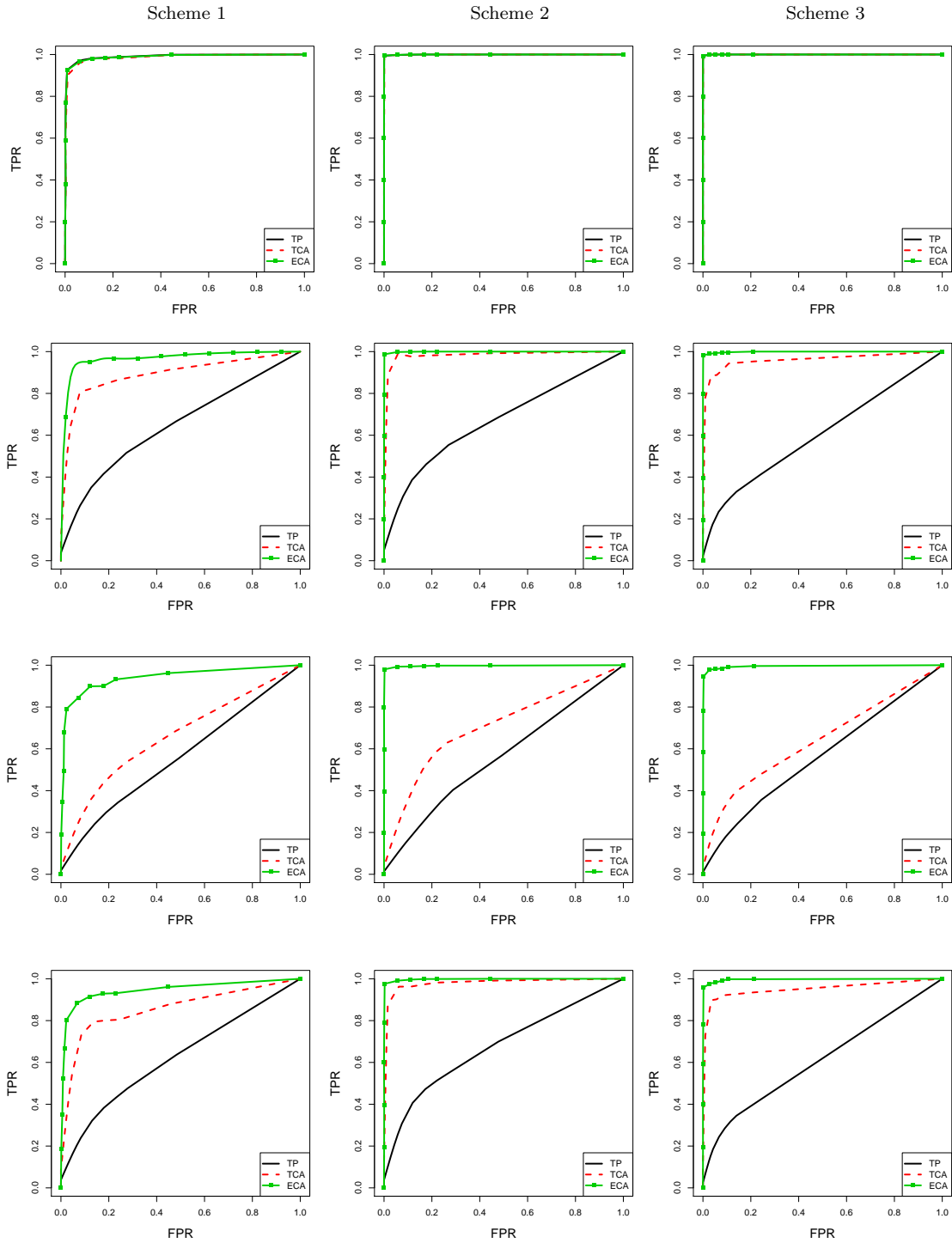


Figure 3: ROC curves for different methods in schemes 1 to 3 and different distributions (normal, multivariate- t , EC1, and EC2, from top to bottom) using the truncated power method. Here we are interested in estimating the leading eigenvector.

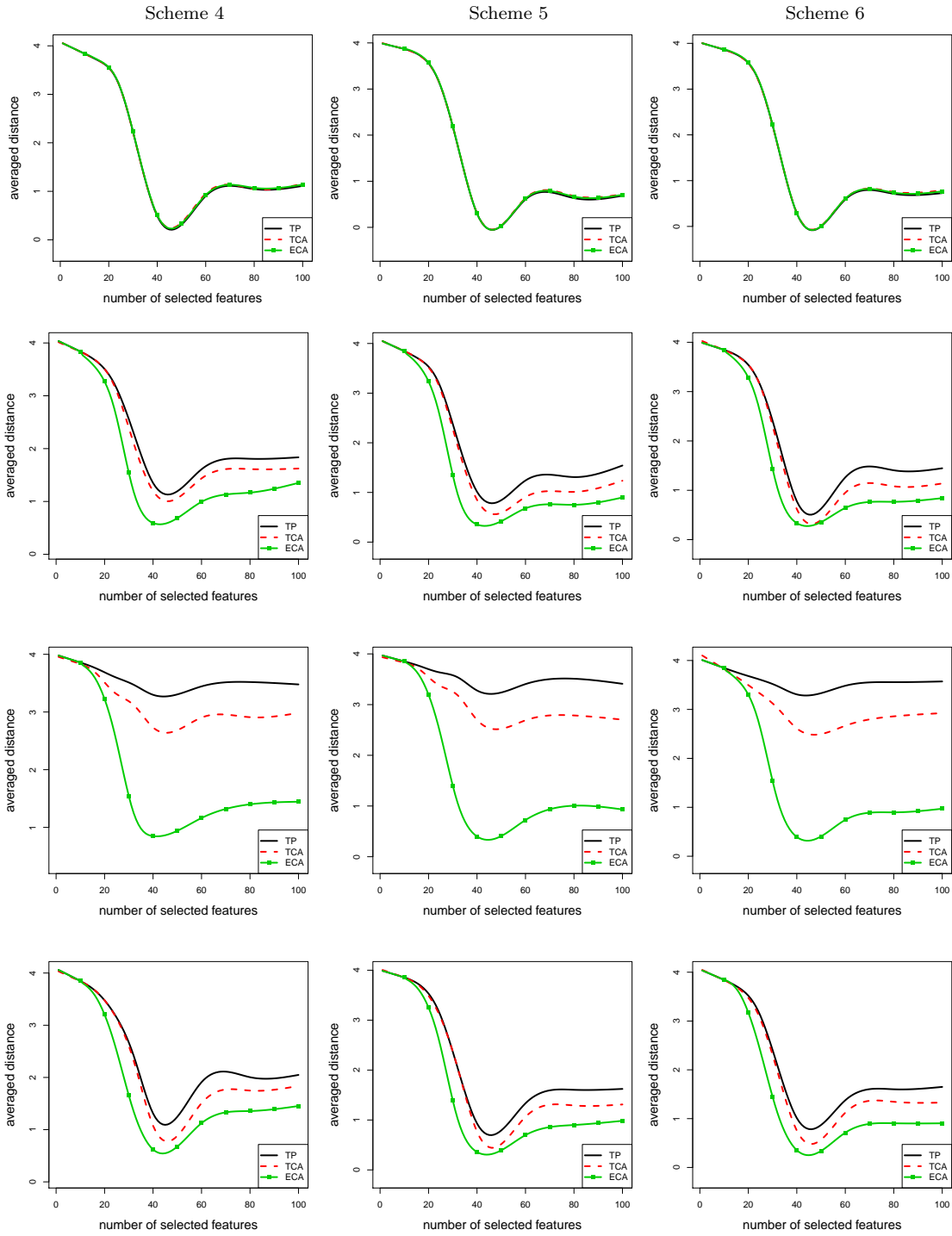


Figure 4: Curves of averaged distances between the estimates and true parameters for different methods in schemes 4 to 6 and different distributions (normal, multivariate- t , EC1, and EC 2, from top to bottom) using the truncated power method. Here we are interested in estimating the top m leading eigenvectors. The horizontal-axis represents the cardinalities of the estimates' support sets and the vertical-axis represents the averaged distances.

Table 2: Quantitative comparison on the dataset under the three schemes 1 to 3 and four different distributions. The means of the $|\sin \angle(\mathbf{u}_1, \hat{\mathbf{u}}_1)|$ with their standard deviations in parentheses are presented.

Distribution	Scheme	TP	TCA	ECA
normal	1	0.3289(0.0422)	0.3699(0.0437)	0.3309(0.0425)
	2	0.1542(0.0169)	0.1606(0.0180)	0.1548(0.0158)
	3	0.1523(0.0181)	0.1584(0.0200)	0.1538(0.0189)
multivariate- t	1	0.9068(0.0415)	0.6420(0.0646)	0.4544(0.0662)
	2	0.8865(0.0547)	0.4098(0.0660)	0.1800(0.0231)
	3	0.9069(0.0445)	0.4633(0.0662)	0.1871(0.0261)
EC1	1	0.9693(0.0131)	0.9088(0.0323)	0.5066(0.0569)
	2	0.9707(0.0130)	0.9069(0.0320)	0.1988(0.02945)
	3	0.9876(0.0072)	0.9425(0.0260)	0.2451(0.0459)
EC2	1	0.9342(0.0282)	0.7335(0.0470)	0.4978(0.0522)
	2	0.8796(0.0448)	0.4273(0.0535)	0.2064(0.0307)
	3	0.9309(0.0371)	0.4702(0.0609)	0.2336(0.0390)

to estimate the eigenvectors $\mathbf{u}_1, \dots, \mathbf{u}_4$. The tuning parameter remains the same in each iterative delation step.

Parallel to the last section, Figure 4 plots the estimated distances between the estimates $\hat{\mathbf{u}}_1, \dots, \hat{\mathbf{u}}_4$ and the true parameters $\mathbf{u}_1, \dots, \mathbf{u}_4$ against the numbers of estimated nonzero entries. Here the distance is defined as $\sum_{j=1}^4 |\sin \angle(\mathbf{u}_j, \hat{\mathbf{u}}_j)|$ and the number is defined as $\sum_{j=1}^4 \|\hat{\mathbf{u}}_j\|_0$. We see that the averaged distance starts from 4 and decreases first and then increases with the number of estimated nonzero entries. The minimum achieves when the number of nonzero entries is 40.

Setting the tuning parameter in each step to be 10, we conduct a quantitative comparison among ECA, TCA, and TP by presenting the averaged distances with standard deviations provided in the parentheses. The same conclusions drawn in the last section hold here, indicating that ECA is a safe alternative to the classical sparse PCA when the data are elliptically distributed.

5.2 Brain Imaging Data Study

In this section we apply ECA and the other two methods to a brain imaging data obtained from the Autism Brain Imaging Data Exchange (ABIDE) project (Di Martino et al., 2013). The ABIDE project shares over 1,000 functional and structural scans with and without

Table 3: Quantitative comparison on the dataset under the schemes 4 to 6 and four different distributions. The means of the $\sum_{j=1}^4 |\sin \angle(\mathbf{u}_j, \hat{\mathbf{u}}_j)|$ with their standard deviations in parentheses are presented.

Distribution	Scheme	TP	TCA	ECA
normal	4	0.4175(0.0476)	0.4347(0.0496)	0.4217(0.0421)
	5	0.2702(0.0225)	0.2825(0.0241)	0.2741(0.0237)
	6	0.2642(0.0215)	0.2721(0.0225)	0.2669(0.0225)
multivariate- <i>t</i>	4	0.7998(0.0904)	0.6843(0.0851)	0.4559(0.0427)
	5	0.5996(0.0608)	0.4446(0.0430)	0.3283(0.0291)
	6	0.5466(0.0638)	0.3991(0.0461)	0.2959(0.0273)
EC1	4	2.6605(0.1432)	1.8830(0.1775)	0.5566(0.0557)
	5	2.6618(0.1370)	1.6285(0.1613)	0.3510(0.0302)
	6	2.7734(0.1255)	1.6392(0.1838)	0.3573(0.0323)
EC2	4	0.9056(0.1150)	0.7301(0.0972)	0.4883(0.0494)
	5	0.6539(0.0785)	0.4803(0.0539)	0.3288(0.0328)
	6	0.6585(0.0843)	0.4469(0.0459)	0.3157(0.0314)

autism. This dataset includes 1,043 subjects, of which 544 are control and the rest are diagnosed with autism. Each subject is scanned for multiple time points, ranging from 72 to 290. The data were pre-processed for correcting the motion and eliminating noises. We refer to Di Martino et al. (2013) and Kang (2013) for more details in data preprocessing procedures.

Based on the 3D scans, we extracted 116 regions that are of interest from the AAL atlas (Tzourio-Mazoyer et al., 2002), and broadly cover the brain. This gives us 1,043 matrices, each with 116 columns and number of rows from 72 to 290. We then followed the idea in Eloyan et al. (2012) and Han et al. (2013) to compress the information of each subject by taking the median of each column for each matrix. In this study, we are mainly interested in studying the control group. This gives us a 544×116 matrix.

First, we explore the obtained matrix to unveil several characteristics of this dataset. In general, we find that the observed data are non-Gaussian and marginally symmetric. We first illustrate the non-Gaussian issue. Table 4 provides the results of marginal normality tests. Here we conduct the three marginal normality tests at the significant level of 0.05. It is clear that at most 28 out of 116 voxels would pass any of three normality test. With Bonferroni correction there are still over half voxels that fail to pass any normality tests. This indicates that the imaging data are not Gaussian distributed.

Table 4: Testing for normality of the ABIDE data. This table illustrates the number of voxels (out of a total number 116) rejecting the null hypothesis of normality at the significance level of 0.05.

Critical value	Kolmogorov-Smirnov	Shapiro-Wilk	Lilliefors
0.05	88	115	115
0.05/116	61	113	92

We then show that the data are marginally symmetric. For this, we first calculate the marginal skewness of each column in the data matrix. We then compare the empirical distribution function based on the marginal skewness values of the data matrix with that based on the simulated data from the standard Gaussian ($N(0, 1)$), t distribution with degree freedom 3 ($t(df = 3)$), t distribution with degree freedom 5 ($t(df = 5)$), and the exponential distribution with the rate parameter 1 ($\exp(1)$). Here the first three distributions are symmetric and the exponential distribution is skewed to the right. Figure 5 plots the five estimated distribution functions. We see that the distribution function for the marginal skewness of the imaging data is very close to that of the t distribution $t(df = 3)$. This indicates that the data are marginally symmetric. Moreover, the distribution function based on the imaging data is far away from that based on the Gaussian distribution, indicating that the data can be heavy-tailed.

The above data exploration results reveal that the ABIDE data are non-Gaussian, symmetric, and heavy-tailed, which make elliptical distribution an very appealing way in modeling the data. We then apply TP, TCA and ECA to this dataset. We extracted the top three eigenvectors and set the tuning parameter of the truncated power method to be 40. We projected any two principal components of the ABIDE data in 2D plots, shown in Figure 6. Here the red dots represent the possible outliers that have strong leverage influence. The leverage strength is defined as the diagonal values of the hat matrix in the linear model by regressing the first principal component on the second one (Neter et al., 1996). High leverage strength means that including these points will severely affect the linear regression estimates applied to principal components of the data. We say that a data point has a strong leverage influence if its leverage strength is higher than a chosen threshold value. Here we chose the threshold value to be $0.05(\approx 27/544)$.

It can be observed that there are points with strong leverage influence for both statistics learnt by TP and TCA, while none for ECA. This implies that ECA has the potential to deliver better results for inference based on the estimated principal components.

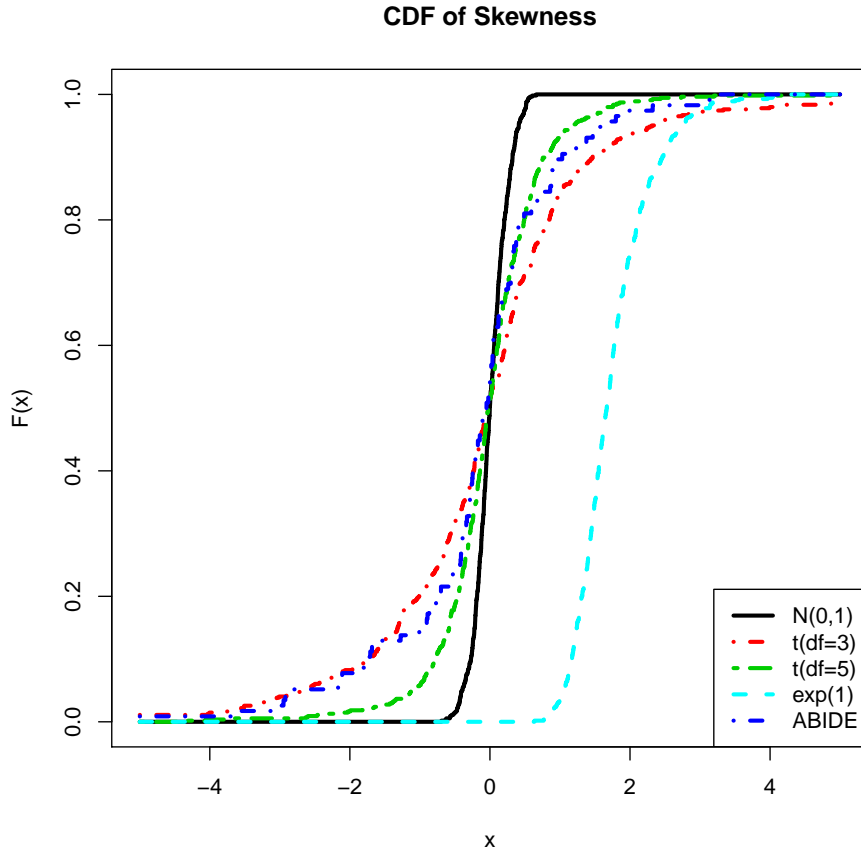


Figure 5: Illustration of the symmetric and heavy-tailed properties of the brain imaging data. The estimated cumulative distribution functions (CDF) of the marginal skewness based on the ABIDE data and four simulated distributions are plotted against each other.

6 Proofs

In this section we provide the proofs of results shown in Section 4. For notational simplicity, in the sequel we assume that the sample size n is even. When n is odd, we can always use $n - 1$ data points without affecting the obtained rate of convergence.

6.1 Proof of Theorem 4.1

To prove Theorem 4.1, we first prove the following lemma, which connects $\sin \angle(\mathbf{u}_1, \hat{\mathbf{u}}_1^*)$ with the restricted spectral norm $\sup_{\mathbf{v} \in \mathbb{S}^{d-1} \cap \mathbb{B}_0(2s)} |\mathbf{v}^T (\mathbf{K} - \hat{\mathbf{K}}) \mathbf{v}|$. In the sequel, we assume that the conditions in Theorem 4.1 hold.

Lemma 6.1 (Vu and Lei (2012)). *Using the notation in Theorem 4.1, \mathbf{u}_1 and $\hat{\mathbf{u}}_1$ satisfy*

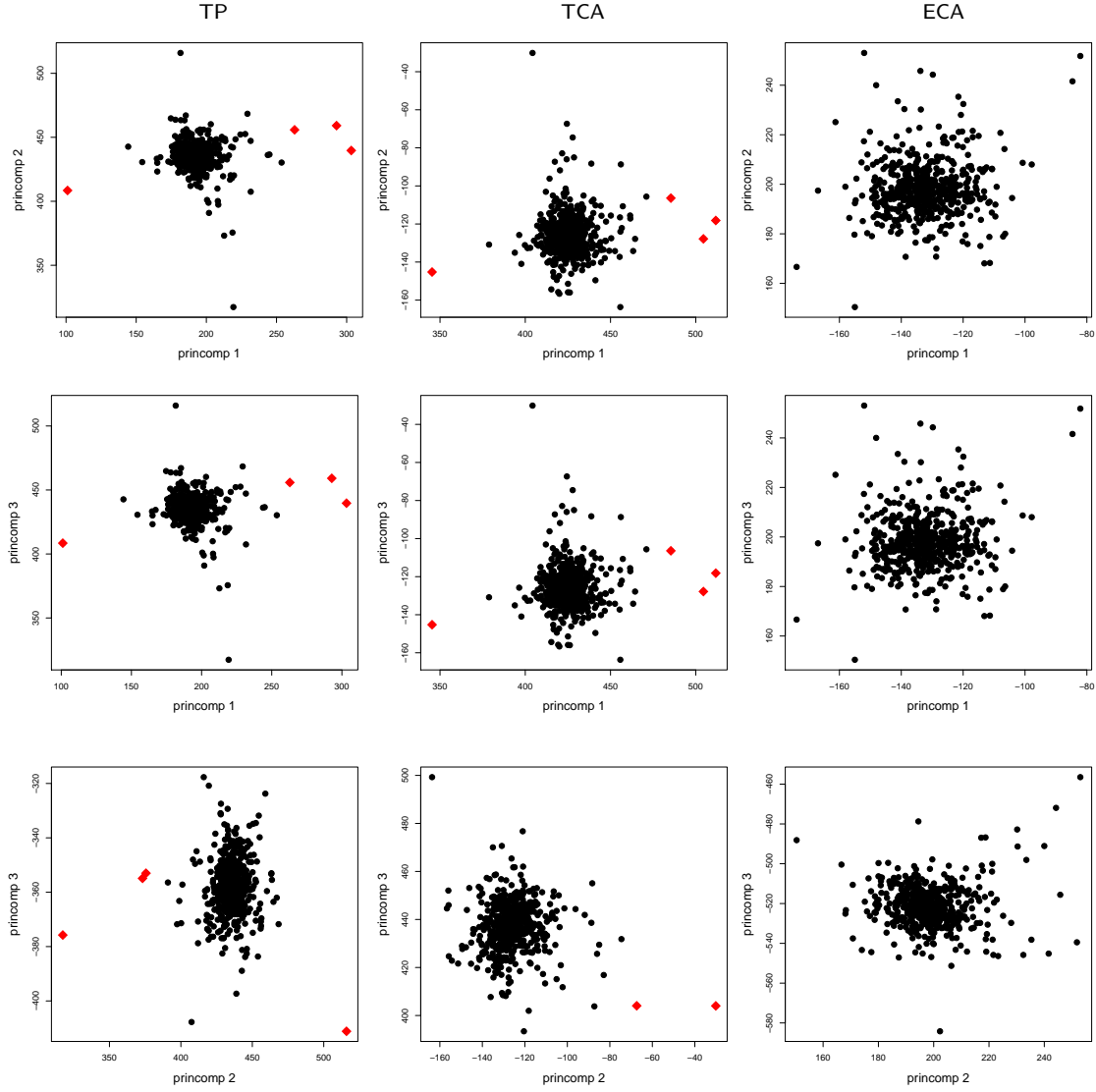


Figure 6: Plots of principal components 1 against 2, 1 against 3, 2 against 3 from top to bottom. The methods used are TP, TCA and ECA. Here red dots represent the points with strong leverage influence.

that

$$|\sin \angle(\mathbf{u}_1, \hat{\mathbf{u}}_1)| \leq \frac{2}{\Lambda_1(\mathbf{K}) - \Lambda_2(\mathbf{K})} \sup_{\mathbf{v} \in \mathbb{S}^{d-1} \cap \mathbb{B}_0(2s)} |\mathbf{v}^T (\mathbf{K} - \hat{\mathbf{K}}) \mathbf{v}|.$$

Proof. Check the proof of Theorem 2.2 in Vu and Lei (2012). \square

We denote $\mathbf{X} \in \mathcal{M}_d(\boldsymbol{\Sigma}, \xi, s; \kappa_L, \kappa_U)$ to be a random vector and $\widetilde{\mathbf{X}}$ to be an independent copy of \mathbf{X} , let $S(\mathbf{X}) := (\mathbf{X} - \widetilde{\mathbf{X}}) / \|\mathbf{X} - \widetilde{\mathbf{X}}\|_2$. The next lemma shows that when $S(\mathbf{X})$

satisfies certain conditions, we have

$$\sup_{\mathbf{v} \in \mathbb{S}^{d-1} \cap \mathbb{B}_0(2s)} \left| \mathbf{v}^T \left(\widehat{\mathbf{K}} - \mathbf{K} \right) \mathbf{v} \right| = O_P \left(\eta^{1/2} \sqrt{\frac{s \log d}{n}} \right),$$

where η only depends on Σ .

Lemma 6.2. *With the notation in Theorem 4.1, for any $\mathbf{v} \in \mathbb{S}^{d-1}$, if*

$$\mathbb{E} \exp \left(t \left[(\mathbf{v}^T S(\mathbf{X}))^2 - \mathbf{v}^T \mathbf{K} \mathbf{v} \right] \right) \leq \exp(\eta t^2), \quad (6.1)$$

where $\eta > 0$ only depends on the eigenvalues of Σ , we have, with probability no smaller than $1 - 2\alpha$,

$$\sup_{\mathbf{v} \in \mathbb{S}^{d-1} \cap \mathbb{B}_0(2s)} \left| \mathbf{v}^T \left(\widehat{\mathbf{K}} - \mathbf{K} \right) \mathbf{v} \right| \leq 2(8\eta)^{1/2} \sqrt{\frac{2s(3 + \log(d/2s)) + \log(1/\alpha)}{n}}. \quad (6.2)$$

Proof. Let $q \in \mathbb{Z}^+$ be an integer larger than 1. Let J_q be any subset of $\{1, \dots, d\}$ with cardinality q . For any $2s$ -dimensional sphere \mathbb{S}^{2s-1} equipped with Euclidean distance, we let \mathcal{N}_ϵ be a subset of \mathbb{S}^{2s-1} such that for any $\mathbf{v} \in \mathbb{S}^{2s-1}$, there exists $\mathbf{u} \in \mathcal{N}_\epsilon$ subject to $\|\mathbf{u} - \mathbf{v}\|_2 \leq \epsilon$. Vershynin (2010) showed that the cardinal number of \mathcal{N}_ϵ has an upper bound

$$\text{card}(\mathcal{N}_\epsilon) < \left(1 + \frac{2}{\epsilon} \right)^{2s}.$$

Let $\mathcal{N}_{1/4}$ be a $(1/4)$ -net of \mathbb{S}^{2s-1} . We then have $\text{card}(\mathcal{N}_{1/4})$ is upper bounded by 9^{2s} . Moreover, for any matrix $\mathbf{M} \in \mathbb{R}^{2s \times 2s}$, we have

$$\sup_{\mathbf{v} \in \mathbb{S}^{2s-1}} |\mathbf{v}^T \mathbf{M} \mathbf{v}| \leq \frac{1}{1 - 2\epsilon} \sup_{\mathbf{v} \in \mathcal{N}_\epsilon} |\mathbf{v}^T \mathbf{M} \mathbf{v}|.$$

This implies that

$$\sup_{\mathbf{v} \in \mathbb{S}^{2s-1}} |\mathbf{v}^T \mathbf{M} \mathbf{v}| \leq 2 \sup_{\mathbf{v} \in \mathcal{N}_{1/4}} |\mathbf{v}^T \mathbf{M} \mathbf{v}|.$$

Let $\beta > 0$ be a quantity defined as

$$\beta := (8\eta)^{1/2} \sqrt{\frac{2s(3 + \log(d/2s)) + \log(1/\alpha)}{n}}.$$

By the union bound, we have

$$\begin{aligned} & \mathbb{P} \left(\sup_{\mathbf{b} \in \mathbb{S}^{2s-1}} \sup_{J_{2s} \subset \{1, \dots, d\}} \left| \mathbf{b}^T \left[\widehat{\mathbf{K}} - \mathbf{K} \right]_{J_{2s}, J_{2s}} \mathbf{b} \right| > 2\beta \right) \\ & \leq \mathbb{P} \left(\sup_{\mathbf{b} \in \mathcal{N}_{1/4}} \sup_{J_{2s} \subset \{1, \dots, d\}} \left| \mathbf{b}^T \left[\widehat{\mathbf{K}} - \mathbf{K} \right]_{J_{2s}, J_{2s}} \mathbf{b} \right| > \beta \right) \\ & \leq 9^{2s} \binom{d}{2s} \mathbb{P} \left(\left| \mathbf{b}^T \left[\widehat{\mathbf{K}} - \mathbf{K} \right]_{J_{2s}, J_{2s}} \mathbf{b} \right| > (8\eta)^{1/2} \sqrt{\frac{2s(3 + \log(d/2s)) + \log(1/\alpha)}{n}}, \right. \\ & \quad \left. \text{for any } \mathbf{b} \text{ and } J_{2s} \right). \end{aligned}$$

Thus, if we can show that for any $\mathbf{b} \in \mathbb{S}^{2s-1}$ and J_{2s} , we have

$$\mathbb{P} \left(\left| \mathbf{b}^T \left[\widehat{\mathbf{K}} - \mathbf{K} \right]_{J_{2s}, J_{2s}} \mathbf{b} \right| > t \right) \leq 2e^{-nt^2/(8\eta)}, \quad (6.3)$$

for η defined in Equation (6.1). Then using the bound $\binom{d}{2s} < \{ed/(2s)\}^{2s}$, we have

$$\begin{aligned} & 9^{2s} \binom{d}{2s} \mathbb{P} \left(\left| \mathbf{b}^T \left[\widehat{\mathbf{K}} - \mathbf{K} \right]_{J_{2s}, J_{2s}} \mathbf{b} \right| > (8\eta)^{1/2} \sqrt{\frac{2s(3 + \log(d/2s)) + \log(1/\alpha)}{n}} \right) \\ & \quad \text{for any } \mathbf{b} \text{ and } J \Big) \\ & \leq 2 \exp\{2s(1 + \log 9 - \log(2s)) + 2s \log d - 2s(3 + \log d - \log(2s)) - \log(1/\alpha)\} \\ & \leq 2\alpha. \end{aligned}$$

It shows that, with probability greater than $1 - 2\alpha$, the bound in Equation (6.2) holds.

We now show that Equation (6.3) holds. For any t , we have

$$\begin{aligned} & \mathbb{E} \exp \left\{ t \cdot \mathbf{b}^T \left[\widehat{\mathbf{K}} - \mathbf{K} \right]_{J_{2s}, J_{2s}} \mathbf{b} \right\} \\ & = \mathbb{E} \exp \left\{ t \cdot \frac{1}{\binom{n}{2}} \sum_{i < i'} \mathbf{b}^T \left(\frac{(\mathbf{x}_i - \mathbf{x}_{i'})_{J_{2s}} (\mathbf{x}_i - \mathbf{x}_{i'})_{J_{2s}}^T}{\|\mathbf{x}_i - \mathbf{x}_{i'}\|_2^2} - \mathbf{K}_{J_{2s}, J_{2s}} \right) \mathbf{b} \right\}. \end{aligned}$$

Let S_n represent the permutation group of $\{1, \dots, n\}$. For any $\sigma \in S_n$, let $(i_1, \dots, i_n) := \sigma(1, \dots, n)$ represent a permuted series of $\{1, \dots, n\}$ and $O(\sigma) := \{(i_1, i_2), (i_3, i_4), \dots, (i_{n-1}, i_n)\}$. In particular, we denote $O(\sigma_0) := \{(1, 2), (3, 4), \dots, (n-1, n)\}$. By simple calculation,

$$\begin{aligned} & \mathbb{E} \exp \left\{ t \cdot \frac{1}{\binom{n}{2}} \sum_{i < i'} \mathbf{b}^T \left(\frac{(\mathbf{x}_i - \mathbf{x}_{i'})_{J_{2s}} (\mathbf{x}_i - \mathbf{x}_{i'})_{J_{2s}}^T}{\|\mathbf{x}_i - \mathbf{x}_{i'}\|_2^2} - \mathbf{K}_{J_{2s}, J_{2s}} \right) \mathbf{b} \right\} \\ & = \mathbb{E} \exp \left\{ t \cdot \frac{1}{\text{card}(S_n)} \sum_{\sigma \in S_n} \frac{2}{n} \sum_{(i, i') \in O(\sigma)} \mathbf{b}^T \left(\frac{(\mathbf{x}_i - \mathbf{x}_{i'})_{J_{2s}} (\mathbf{x}_i - \mathbf{x}_{i'})_{J_{2s}}^T}{\|\mathbf{x}_i - \mathbf{x}_{i'}\|_2^2} - \mathbf{K}_{J_{2s}, J_{2s}} \right) \mathbf{b} \right\} \\ & \leq \frac{1}{\text{card}(S_n)} \sum_{\sigma \in S_n} \mathbb{E} \exp \left\{ t \cdot \frac{2}{n} \sum_{(i, i') \in O(\sigma)} \mathbf{b}^T \left(\frac{(\mathbf{x}_i - \mathbf{x}_{i'})_{J_{2s}} (\mathbf{x}_i - \mathbf{x}_{i'})_{J_{2s}}^T}{\|\mathbf{x}_i - \mathbf{x}_{i'}\|_2^2} - \mathbf{K}_{J_{2s}, J_{2s}} \right) \mathbf{b} \right\} \\ & = \mathbb{E} \exp \left\{ t \cdot \frac{2}{n} \sum_{(i, i') \in O(\sigma_0)} \mathbf{b}^T \left(\frac{(\mathbf{x}_i - \mathbf{x}_{i'})_{J_{2s}} (\mathbf{x}_i - \mathbf{x}_{i'})_{J_{2s}}^T}{\|\mathbf{x}_i - \mathbf{x}_{i'}\|_2^2} - \mathbf{K}_{J_{2s}, J_{2s}} \right) \mathbf{b} \right\}, \quad (6.4) \end{aligned}$$

where inequality is due to the Jensen's inequality.

Let $m := n/2$ and recall that $\mathbf{X} = (X_1, \dots, X_d)^T \in \mathcal{M}_d(\boldsymbol{\Sigma}, \xi, s; \kappa_L, \kappa_U)$, let $\widetilde{\mathbf{X}} = (\widetilde{X}_1, \dots, \widetilde{X}_d)^T$ be an independent copy of \mathbf{X} , by Equation (6.1), we have that, for any

$t \in \mathbb{R}$ and $\mathbf{v} \in \mathbb{S}^{d-1}$,

$$\mathbb{E} \exp \left[t \cdot \mathbf{v}^T \left(\frac{(\mathbf{X} - \widetilde{\mathbf{X}})(\mathbf{X} - \widetilde{\mathbf{X}})}{\|\mathbf{X} - \widetilde{\mathbf{X}}\|_2^2} - \mathbf{K} \right) \mathbf{v} \right] \leq e^{\eta t^2}.$$

In particular, letting $\mathbf{v}_{J_{2s}} = \mathbf{b}$ and $\mathbf{v}_{J_{2s}^c} = \mathbf{0}$, we have

$$\mathbb{E} \exp \left\{ t \mathbf{b}^T \left(\frac{(\mathbf{X} - \widetilde{\mathbf{X}})_{J_{2s}} (\mathbf{X} - \widetilde{\mathbf{X}})_{J_{2s}}^T}{\|\mathbf{X} - \widetilde{\mathbf{X}}\|_2^2} - \mathbf{K}_{J_{2s}, J_{2s}} \right) \mathbf{b} \right\} \leq e^{\eta t^2}. \quad (6.5)$$

Then we are able to continue Equation (6.4) as

$$\begin{aligned} & \mathbb{E} \exp \left\{ t \cdot \frac{2}{n} \sum_{(i, i') \in O(\sigma_0)} \mathbf{b}^T \left(\frac{(\mathbf{x}_i - \mathbf{x}_{i'})_{J_{2s}} (\mathbf{x}_i - \mathbf{x}_{i'})_{J_{2s}}^T}{\|\mathbf{x}_i - \mathbf{x}_{i'}\|_2^2} - \mathbf{K}_{J_{2s}, J_{2s}} \right) \mathbf{b} \right\} \\ &= \mathbb{E} \exp \left\{ \frac{t}{m} \sum_{i=1}^m \mathbf{b}^T \left(\frac{(\mathbf{x}_{2i} - \mathbf{x}_{2i-1})_{J_{2s}} (\mathbf{x}_{2i} - \mathbf{x}_{2i-1})_{J_{2s}}^T}{\|\mathbf{x}_{2i} - \mathbf{x}_{2i-1}\|_2^2} - \mathbf{K}_{J_{2s}, J_{2s}} \right) \mathbf{b} \right\} \\ &= \left(\mathbb{E} e^{\frac{t}{m} ((\mathbf{b}^T S(\mathbf{X})_{J_{2s}})^2 - \mathbf{b}^T \mathbf{K}_{J_{2s}, J_{2s}} \mathbf{b})} \right)^m \\ &\leq e^{\eta t^2 / m}, \end{aligned} \quad (6.6)$$

where by Equation (6.1), the last inequality holds for any t . Accordingly, choosing $t = \beta m / (2\eta)$, using the Markov inequality, we have

$$\mathbb{P} \left(\mathbf{b}^T \left[\widehat{\mathbf{K}} - \mathbf{K} \right]_{J_{2s}, J_{2s}} \mathbf{b} > \beta \right) \leq e^{-n\beta^2 / (8\eta)}. \quad (6.7)$$

By symmetry, we have the same bound for $\mathbb{P} \left(\mathbf{b}^T \left[\widehat{\mathbf{K}} - \mathbf{K} \right]_{J_{2s}, J_{2s}} \mathbf{b} < -\beta \right)$ as in Equation (6.7). Together, they give us Equation (6.3). This completes the proof. \square

The next lemma calculates the exact value of η in Equation (6.1) under the conditions of Theorem 4.1.

Lemma 6.3. *Under the conditions of Theorem 4.1, Equation (6.1) holds with*

$$\eta = C_3 \left\{ \frac{C_2}{d-2} + \Lambda_1(\mathbf{K}) \right\}^2,$$

where C_2 and C_3 are two absolute constants.

Proof. Remind that for any $\mathbf{X} \in \mathcal{M}_d(\boldsymbol{\Sigma}, \xi, s; \kappa_L, \kappa_U)$, $S(\mathbf{X})$ is defined as:

$$S(\mathbf{X}) = \frac{\mathbf{X} - \widetilde{\mathbf{X}}}{\|\mathbf{X} - \widetilde{\mathbf{X}}\|_2} \stackrel{d}{=} \frac{\mathbf{X}^*}{\|\mathbf{X}^*\|_2} \stackrel{d}{=} \frac{\mathbf{Z}^0}{\|\mathbf{Z}^0\|_2},$$

where $\mathbf{X}^* \sim EC_d(\mathbf{0}, \mathbf{\Sigma}, \xi^*)$ for some random variable $\xi^* \geq 0$ with $\mathbb{P}(\xi^* = 0) = 0$ and $\mathbf{Z}^0 \sim N_d(\mathbf{0}, \mathbf{\Sigma})$. Here the second equality is due to the fact that the summation of two independent elliptically distributed random vectors follows an elliptical distribution (see Lemma 1 in Lindskog et al. (2003) for a proof). The third equality holds because $\mathbf{X}^* \stackrel{d}{=} \xi' \mathbf{Z}^0$ for some random variable $\xi' \geq 0$ with $\mathbb{P}(\xi' = 0) = 0$. Therefore, to prove Equation (6.1) holds, we only need to focus on

$$\frac{\mathbf{Z}^0}{\|\mathbf{Z}^0\|_2} \stackrel{d}{=} S(\mathbf{X}).$$

For any $\mathbf{v}_1 \in \mathbb{S}^{d-1}$, using the basis expansion theorem (Trefethen and Bau III, 1997), we can construct a set of basis $\mathbf{v}_2, \mathbf{v}_3, \dots, \mathbf{v}_d$ such that, combined with \mathbf{v}_1 , satisfying that for any $i \neq j \in \{1, \dots, d\}$,

$$\|\mathbf{v}_i\|_2 = 1, \quad \mathbf{v}_i^T \mathbf{\Sigma} \mathbf{v}_j = 0, \quad \text{and} \quad \Lambda_d(\mathbf{\Sigma}) \leq \mathbf{v}_i^T \mathbf{\Sigma} \mathbf{v}_i \leq \Lambda_1(\mathbf{\Sigma}). \quad (6.8)$$

Letting $\mathbf{V} := [\mathbf{v}_1, \dots, \mathbf{v}_d] \in \mathbb{R}^{d \times d}$, we have, for any $\mathbf{v} \in \mathbb{S}^{d-1}$ and $\mathbf{u} := \mathbf{\Sigma}^{-1/2} \mathbf{v}$,

$$\mathbf{v}^T \mathbf{V} \mathbf{V}^T \mathbf{v} = \mathbf{u}^T \mathbf{\Sigma}^{1/2} \mathbf{V} \mathbf{V}^T \mathbf{\Sigma}^{1/2} \mathbf{u}.$$

For $i = 1, \dots, d$, letting $\boldsymbol{\theta}_i := \mathbf{\Sigma}^{1/2} \mathbf{v}_i$, by definition of $\mathbf{v}_2, \dots, \mathbf{v}_d$, we have $\boldsymbol{\theta}_i^T \boldsymbol{\theta}_i = \mathbf{v}_i^T \mathbf{\Sigma} \mathbf{v}_i$ and $\boldsymbol{\theta}_i^T \boldsymbol{\theta}_j = 0$ for any $j \neq i$. Accordingly, we have $\mathbf{\Sigma}^{1/2} \mathbf{V} = [\boldsymbol{\theta}_1, \dots, \boldsymbol{\theta}_d]$ and

$$\mathbf{u}^T \mathbf{\Sigma}^{1/2} \mathbf{V} \mathbf{V}^T \mathbf{\Sigma}^{1/2} \mathbf{u} = \mathbf{u}^T \left(\sum_i \boldsymbol{\theta}_i \boldsymbol{\theta}_i^T \right) \mathbf{u} \leq \|\mathbf{u}\|_2^2 \max_i (\mathbf{v}_i^T \mathbf{\Sigma} \mathbf{v}_i) \leq \frac{\Lambda_1(\mathbf{\Sigma})}{\Lambda_d(\mathbf{\Sigma})} \leq \kappa_U.$$

This implies that

$$\|\mathbf{V} \mathbf{V}^T\|_2 \leq \kappa_U \Rightarrow \|\mathbf{V}^T \mathbf{Z}^0\|_2 \leq \kappa_U^{1/2} \|\mathbf{Z}^0\|_2.$$

We then have that

$$|\mathbf{v}_1^T S(\mathbf{X})| \stackrel{d}{=} \frac{|\mathbf{v}_1^T \mathbf{Z}^0|}{\|\mathbf{Z}^0\|_2} \leq \kappa_U^{1/2} \cdot \frac{|\mathbf{v}_1^T \mathbf{Z}^0|}{\|\mathbf{V}^T \mathbf{Z}^0\|_2} = \kappa_U^{1/2} \cdot \frac{\sigma_1 |Y_1|}{\sqrt{\sum_{i=1}^d \sigma_i^2 Y_i^2}},$$

where for $i = 1, \dots, d$, we define $Y_i := \mathbf{v}_i^T \mathbf{Z}^0 / \sqrt{\mathbf{v}_i^T \mathbf{\Sigma} \mathbf{v}_i}$ and $\sigma_i := \sqrt{\mathbf{v}_i^T \mathbf{\Sigma} \mathbf{v}_i}$. Noticing that $(Y_1, \dots, Y_d)^T$ is a linear transformation of \mathbf{Z}^0 and accordingly are Gaussian distributed, and for any $i \neq j$,

$$\text{cov}(Y_i, Y_j) = \mathbf{v}_i^T \mathbf{\Sigma} \mathbf{v}_j = 0,$$

we have Y_1, \dots, Y_d are independent of each other. This implies that for any parameter $u > 0$,

$$\begin{aligned} \mathbb{E} \exp(u(\mathbf{v}_1^T S(\mathbf{X}))^4) &\leq \kappa_U^2 \cdot \mathbb{E} \exp \left\{ u \left(\frac{\sigma_1^2 Y_1^2}{\sum_{i=1}^n \sigma_i^2 Y_i^2} \right)^2 \right\} \\ &= \kappa_U^2 \cdot \mathbb{E} \exp \left\{ u \left(\frac{Y_1^2}{\sum_{i=1}^n (\sigma_i^2 / \sigma_1^2) Y_i^2} \right)^2 \right\} \\ &\leq \kappa_U^2 \cdot \mathbb{E} \exp \left\{ u \cdot \frac{\sigma_1^4}{\sigma_d^4} \left(\frac{Y_1^2}{\sum_{i=1}^n Y_i^2} \right)^2 \right\}. \end{aligned}$$

Using Equation (6.8) and the fact that $\Lambda_1(\boldsymbol{\Sigma}) \leq \kappa_U \Lambda_d(\boldsymbol{\Sigma})$, we have there exists a fixed constant κ such that

$$\frac{\sigma_1^4}{\sigma_d^4} \leq \frac{\Lambda_1(\boldsymbol{\Sigma})^2}{\Lambda_d(\boldsymbol{\Sigma})^2} \leq \kappa_U^2.$$

Therefore, we have

$$\begin{aligned} \mathbb{E} \exp \left\{ u \cdot \frac{\sigma_1^4}{\sigma_d^4} \left(\frac{Y_1^2}{\sum_{i=1}^n Y_i^2} \right)^2 \right\} &\leq \mathbb{E} \exp \left\{ u \kappa_U^4 \left(\frac{Y_1^2}{\sum_{i=1}^n Y_i^2} \right)^2 \right\} \\ &= \mathbb{E} \exp \left\{ u \kappa_U^4 \left(1 + \frac{Y_2^2 + \dots + Y_d^2}{Y_1^2} \right)^{-2} \right\} \\ &= \mathbb{E} \exp \left\{ u \kappa_U^4 \left(1 + \left(\frac{Y_1^2}{Y_2^2 + \dots + Y_d^2} \right)^{-1} \right)^{-2} \right\}. \end{aligned}$$

Using the concavity of the function $\exp(c(1+x^{-1})^{-2})$, by Jensen's inequality, we have

$$\mathbb{E} \exp \left\{ u \kappa_U^4 \left(1 + \left(\frac{Y_1^2}{Y_2^2 + \dots + Y_d^2} \right)^{-1} \right)^{-2} \right\} \leq \exp \left(u \kappa_U^4 \left[1 + \left\{ \mathbb{E} \left(\frac{Y_1^2}{Y_2^2 + \dots + Y_d^2} \right) \right\}^{-1} \right]^{-2} \right).$$

Because $(d-1)Y_1^2/(Y_2^2 + \dots + Y_d^2) \sim F_{1,d-1}$ follows an F distribution with parameters 1 and $d-1$, we have

$$\mathbb{E} \left(\frac{Y_1^2}{Y_2^2 + \dots + Y_d^2} \right) = \frac{1}{d-3},$$

implying that

$$\begin{aligned} \exp \left(u \kappa_U^4 \left[1 + \left\{ \mathbb{E} \left(\frac{Y_1^2}{Y_2^2 + \dots + Y_d^2} \right) \right\}^{-1} \right]^{-2} \right) &\leq \exp \left(u \kappa_U^4 [1 + d - 3]^{-2} \right) \\ &= \exp(u \kappa_U^4 / (d-2)^2). \end{aligned} \quad (6.9)$$

For any random variable $X \in \mathbb{R}$, we define the subgaussian norm as

$$\|X\|_{\psi_2} := \sup_{k \geq 1} k^{-1/2} (\mathbb{E}|X|^k)^{1/k}.$$

By the definition of the subgaussian random variable and its equivalent conditions shown in pages 10 to 11 in Vershynin (2010), combined with Equation (6.9), we have that there exists a fixed constant C_2 only depending on κ_U such that

$$\|(\mathbf{v}_1^T S(\mathbf{X}))^2\|_{\psi_2} \leq C_2 / (d-2).$$

This implies that

$$\begin{aligned} \|(\mathbf{v}_1^T S(\mathbf{X}))^2 - \mathbf{v}_1^T \mathbf{K} \mathbf{v}_1\|_{\psi_2} &\leq \|(\mathbf{v}_1^T S(\mathbf{X}))^2\|_{\psi_2} + \|\mathbf{v}_1^T \mathbf{K} \mathbf{v}_1\|_{\psi_2} \\ &\leq \frac{C_2}{d-2} + \Lambda_1(\mathbf{K}). \end{aligned}$$

Using the equivalence between Equation (5.11) and (5.12) in Vershynin (2010), we then have, for all $t \in \mathbb{R}$ and fixed $\mathbf{v}_1 \in \mathbb{S}^{d-1}$,

$$\mathbb{E} \exp(t((\mathbf{v}_1^T S(\mathbf{X}))^2 - \mathbf{v}_1^T \mathbf{K} \mathbf{v}_1)) \leq \exp \left[C_3 \left\{ \frac{C_2}{d-2} + \Lambda_1(\mathbf{K}) \right\}^2 \cdot t^2 \right],$$

where C_3 is an absolute constant. This finishes the proof. \square

Proof of Theorem 4.1. Combining the results in Lemmas 6.1 and 6.2, we have that with probability larger than $1 - 2\alpha$,

$$|\sin \angle(\hat{\mathbf{u}}_1^*, \mathbf{u}_1)| \leq \frac{8}{\Lambda_1(\mathbf{K}) - \Lambda_2(\mathbf{K})} \left((2\eta)^{1/2} \sqrt{\frac{2s(3 + \log(d/2s)) + \log(1/\alpha)}{n}} \right).$$

Under the conditions in Theorem 4.1, using Lemma 6.3, we have with probability larger than $1 - 2\alpha$,

$$|\sin \angle(\hat{\mathbf{u}}_1^*, \mathbf{u}_1)| \leq \frac{8\sqrt{2C_3}(C_2/(d-2) + \Lambda_1(\mathbf{K}))}{\Lambda_1(\mathbf{K}) - \Lambda_2(\mathbf{K})} \sqrt{\frac{2s(3 + \log(d/2s)) + \log(1/\alpha)}{n}}. \quad (6.10)$$

Moreover, because $\Lambda_1(\boldsymbol{\Sigma}) \leq \kappa_U \Lambda_d(\boldsymbol{\Sigma}) \Rightarrow \Lambda_1(\boldsymbol{\Sigma}) \leq \kappa_U \Lambda_j(\boldsymbol{\Sigma})$ for any $j \in \{2, \dots, d\}$. Using Equation (3.2), we have,

$$\Lambda_1(\mathbf{K}) = \mathbb{E} \left(\frac{\Lambda_1(\boldsymbol{\Sigma}) U_1^2}{\Lambda_1(\boldsymbol{\Sigma}) U_1^2 + \dots + \Lambda_d(\boldsymbol{\Sigma}) U_d^2} \right) \leq \mathbb{E} \left(\frac{U_1^2}{\sum_{k=1}^d \kappa_U^{-1} U_k^2} \right) = \kappa_U \cdot \frac{1}{d}. \quad (6.11)$$

Similarly, we have

$$\begin{aligned} \Lambda_1(\mathbf{K}) - \Lambda_2(\mathbf{K}) &= \mathbb{E} \left(\frac{\Lambda_1(\boldsymbol{\Sigma}) U_1^2 - \Lambda_2(\boldsymbol{\Sigma}) U_2^2}{\Lambda_1(\boldsymbol{\Sigma}) U_1^2 + \dots + \Lambda_d(\boldsymbol{\Sigma}) U_d^2} \right) \\ &= \mathbb{E} \left(\frac{U_1^2 - \Lambda_2(\boldsymbol{\Sigma})/\Lambda_1(\boldsymbol{\Sigma}) U_2^2}{U_1^2 + \Lambda_2(\boldsymbol{\Sigma})/\Lambda_1(\boldsymbol{\Sigma}) U_2^2 \dots + \Lambda_d(\boldsymbol{\Sigma})/\Lambda_1(\boldsymbol{\Sigma}) U_d^2} \right). \end{aligned}$$

Therefore, using the fact that $\Lambda_1(\boldsymbol{\Sigma}) \geq \kappa_L \Lambda_2(\boldsymbol{\Sigma})$, we have

$$\begin{aligned} \Lambda_1(\mathbf{K}) - \Lambda_2(\mathbf{K}) &= \mathbb{E} \left(\frac{U_1^2 - \Lambda_2(\boldsymbol{\Sigma})/\Lambda_1(\boldsymbol{\Sigma}) U_2^2}{U_1^2 + \Lambda_2(\boldsymbol{\Sigma})/\Lambda_1(\boldsymbol{\Sigma}) U_2^2 \dots + \Lambda_d(\boldsymbol{\Sigma})/\Lambda_1(\boldsymbol{\Sigma}) U_d^2} \right) \\ &\geq \mathbb{E} \left(\frac{U_1^2 - \kappa_L^{-1} U_2^2}{U_1^2 + \dots + U_d^2} \right) \\ &= \mathbb{E}(U_1^2 - \kappa_L^{-1} U_2^2) \\ &= (1 - \kappa_L^{-1}) d^{-1}. \end{aligned} \quad (6.12)$$

Plugging Equations (6.11) and (6.12) into (6.10), for $d \geq 3$, we have with probability larger than $1 - 2\alpha$,

$$|\sin \angle(\hat{\mathbf{u}}_1^*, \mathbf{u}_1)| \leq \frac{8\sqrt{2C_3}(3C_2 + \kappa_U)}{1 - \kappa_L^{-1}} \sqrt{\frac{2s(3 + \log(d/2s)) + \log(1/\alpha)}{n}}. \quad (6.13)$$

This finishes the proof. \square

6.2 Proofs of the Rest Results in Section 4

In this section we provide the rest results in Section 4, including Corollaries 4.2, 4.3, and Theorem 4.4.

Proof of Corollary 4.2. We define $\epsilon = \sin \angle(\tilde{\boldsymbol{\theta}}_1, \boldsymbol{\theta}_1)$. Because $\sin^2(\cdot) \in [0, 1]$, using Theorem 4.1 and choosing $\alpha = 1/n$, we have

$$\begin{aligned} \mathbb{E}\epsilon^2 &= \mathbb{E} \left[\epsilon^2 \cdot I \left(\epsilon^2 < K^2 \cdot \frac{2s(3 + \log(d/2s)) + \log n}{n} \right) \right] + \\ &\quad \mathbb{E} \left[\epsilon^2 \cdot I \left(\epsilon^2 \geq K^2 \cdot \frac{2s(3 + \log(d/2s)) + \log n}{n} \right) \right] \\ &\leq K^2 \cdot \frac{2s(3 + \log(d/2s)) + \log n}{n} + \frac{2}{n}. \end{aligned}$$

This completes the proof. □

Proof of Corollary 4.3. Without loss of generality, we may assume that $\mathbf{u}_1^T \hat{\mathbf{u}}_1^* \geq 0$, because otherwise we can simply conduct appropriate sign changes in the proof. We first note that $s \geq \text{card}(\Upsilon)$. If $\Upsilon \not\subset \hat{\Upsilon}$, then $\Upsilon/\hat{\Upsilon} \neq \emptyset$. This implies that,

$$\|\hat{\mathbf{u}}_1^* - \mathbf{u}_1\|_2 \geq \|(\hat{\mathbf{u}}_1^* - \mathbf{u}_1)_{\Theta/\hat{\Theta}}\|_2 \geq \min_{j \in \Upsilon} |u_{1j}| \geq \sqrt{2}K \cdot \sqrt{\frac{2s(3 + \log(d/2s)) + \log(1/\alpha)}{n}}.$$

We then have

$$\sin^2 \angle(\hat{\mathbf{u}}_1^*, \mathbf{u}_1) = 1 - (\mathbf{u}_1^T \hat{\mathbf{u}}_1^*)^2 \geq 1 - \mathbf{u}_1^T \hat{\mathbf{u}}_1^* = \frac{\|\mathbf{u}_1 - \hat{\mathbf{u}}_1^*\|_2^2}{2},$$

implying that

$$|\sin \angle(\hat{\mathbf{u}}_1^*, \mathbf{u}_1)| \geq \frac{\|\hat{\mathbf{u}}_1^* - \mathbf{u}_1\|_2}{\sqrt{2}} \geq \frac{\min_{j \in \Upsilon} |u_{1j}|}{\sqrt{2}} = K \sqrt{\frac{2s(3 + \log(d/2s)) + \log(1/\alpha)}{n}}. \quad (6.14)$$

Therefore, applying Theorem 4.1, we get

$$\mathbb{P}(\Upsilon \not\subset \hat{\Upsilon}) \leq \mathbb{P} \left(|\sin \angle(\hat{\mathbf{u}}_1^*, \mathbf{u}_1)| \geq K \cdot \sqrt{\frac{2s(3 + \log(d/2s)) + \log(1/\alpha)}{n}} \right) \leq 2\alpha. \quad (6.15)$$

This completes the proof. □

Proof of Theorem 4.4. As shown in the proof of Theorem 4 in Yuan and Zhang (2013), we only need to show that

$$\sup_{\mathbf{v} \in \mathbb{S}^{d-1} \cap \mathbb{B}_0(s)} \left| \mathbf{v}^T \left(d\hat{\mathbf{K}} - d\mathbf{K} \right) \mathbf{v} \right| = O_P \left(\sqrt{\frac{s \log d}{n}} \right),$$

for proving Theorem 4.4. By checking Equation (6.10), we have, with probability larger than $1 - 2\alpha$,

$$\sup_{\mathbf{v} \in \mathbb{S}^{d-1} \cap \mathbb{B}_0(s)} \left| \mathbf{v}^T \left(d\widehat{\mathbf{K}} - d\mathbf{K} \right) \mathbf{v} \right| \leq 8d\sqrt{2C_3}(C_2/(d-2) + \Lambda_1(\mathbf{K}))\sqrt{\frac{s(3 + \log(d/s)) + \log(1/\alpha)}{n}}. \quad (6.16)$$

By checking Equation (6.11), we have

$$\Lambda_1(\mathbf{K}) \leq \kappa_U \cdot \frac{1}{d} \Rightarrow 8d\sqrt{2C_3}(C_2/(d-2) + \Lambda_1(\mathbf{K})) \leq 8\sqrt{2C_3}(3C_2 + \kappa_U). \quad (6.17)$$

Combining Equations (6.16) and (6.17), we get the desired result. \square

7 Conclusion and Discussion

In this paper we propose a new sparse principal component analysis method for high dimensional elliptical models. Our estimator is semiparametric but attains the optimal parametric rate of convergence in parameter estimation. Therefore, compared with the classical sparse PCA, the extra modeling flexibility of the new estimator comes at almost no cost of statistical efficiency.

All existing theoretical analysis on multivariate Kendall's tau has been confined in the low dimensional settings. See for example, Marden (1999), Croux et al. (2002), and Jackson and Chen (2004). To the best of our knowledge, this paper provides the first method as well as theoretical analysis that generalizes this statistic to the high dimensional settings. Our proof techniques for high dimensional minimax optimality is fundamentally different from the previous low-dimensional analysis, which is built under the Le Cam's framework where the dimension d is fixed.

Vu and Lei (2012, 2013) considered sparse principal component analysis and studied the rates of convergence in parameter estimation and minimax estimation under various sparsity assumptions on the leading eigenvectors. Our approach differs from theirs in mainly two aspects: (i) Their analysis relies heavily on the sub-gaussian assumption, which no longer holds under the elliptical model; (ii) They use the Pearson's sample covariance matrix as the algorithm input, while we suggest to use the multivariate Kendall's tau matrix in the elliptical model.

Ma (2013) and Cai et al. (2013) considered sparse principal component analysis under a spiked covariance model. Our approach is fundamentally different from theirs in two aspects: (i) Their analysis relies upon the spiked covariance model and Gaussian assumption, while ECA relaxes both; (ii) Similar to Vu and Lei (2012, 2013), their method requires the Pearson's sample covariance matrix as input, which is not efficient under the elliptical model.

Two other related methods, named TCA and COCA, have been recently proposed by Han and Liu (2013) and Han and Liu (2012), in which they studied the sparse PCA on the transelliptical and nonparanormal models. By using the marginal rank-based estimators (including Kendall’s tau and Spearman’s rho), their methods can obtain efficient estimators for estimating the leading eigenvectors of the (latent) correlation matrix. However, ECA is fundamentally different from TCA and COCA. The main differences between ECA and TCA can be elaborated in three aspects: (i) TCA can only estimate the leading eigenvectors of the correlation matrix, while ECA estimates the leading eigenvectors of the covariance matrix; (ii) Unlike ECA, TCA cannot estimate the principal components; (iii) ECA has a faster convergence rate compared with TCA under elliptical models. On the other hand, ECA is significantly different from COCA in two aspects: (i) COCA assumes the nonparanormal model while ECA assumes the elliptical model. In fact, the only distribution that is shared between the nonparanormal and elliptical families is Gaussian (Liu et al., 2012); (ii) To estimate the leading eigenvectors of the covariance matrix, COCA requires a strong marginal subgaussian assumption, which is not needed for ECA.

Future work includes analyzing the robustness property of the method to more noisy and time series data.

A A Computationally Tractable ECA Algorithm

In this section we provide the ECA algorithm using the truncated power method. The truncated power method is provided in Yuan and Zhang (2013) and the ECA algorithm described here can be regarded as a special application of the truncated power method by using $d\widehat{\mathbf{K}}$ as the input matrix. Before proceeding to the main algorithm, we first introduce an extra notation. For any vector $\mathbf{v} \in \mathbb{R}^d$ and an index set $J \subset \{1, \dots, d\}$, we define the truncation function $\text{TRC}(\cdot, \cdot)$ to be

$$\text{TRC}(\mathbf{v}, J) := (v_1 \cdot I(1 \in J), \dots, v_d \cdot I(d \in J))^T, \quad (\text{A.1})$$

where $I(\cdot)$ is the indicator function. Algorithm 1 provides the detailed algorithm.

To estimate the top m , instead of the top one, leading eigenvectors, we exploit the deflation method proposed in Mackey (2009). In detail, for any positive semidefinite matrix $\mathbf{M} \in \mathbb{R}^{d \times d}$, we define its deflation with regard to $\mathbf{v} \in \mathbb{R}^d$ as:

$$\mathbf{D}(\mathbf{M}, \mathbf{v}) := (\mathbf{I}_d - \mathbf{v}\mathbf{v}^T)\mathbf{M}(\mathbf{I}_d - \mathbf{v}\mathbf{v}^T).$$

In this way, we exploit the following approach to estimate $\mathbf{u}_1, \dots, \mathbf{u}_m$: (i) The estimate $\tilde{\mathbf{u}}_1$ is calculated using Algorithm 1; (ii) Given $\tilde{\mathbf{u}}_1, \dots, \tilde{\mathbf{u}}_j$, we estimate $\tilde{\mathbf{u}}_{j+1}$ by using $\mathbf{M}^{(j+1)} := \mathbf{D}(\mathbf{M}^{(j)}, \tilde{\mathbf{u}}_j)$ as the input matrix to Algorithm 1 ($\mathbf{M}^{(1)} := d\widehat{\mathbf{K}}$).

Algorithm 1 Truncated Power Method

Input: : Multivariate Kendall’s tau matrix $d\widehat{\mathbf{K}}$, initial vector $\mathbf{v}^{(0)} \in \mathbb{S}^{d-1}$, and s as the tuning parameter.

Output: : $\tilde{\mathbf{u}}_1 := \mathbf{v}^{(\infty)}$

Set $t = 1$.

repeat

 Compute $\mathbf{x}_t = d\widehat{\mathbf{K}}\mathbf{v}^{(t-1)}$

if $\|\mathbf{x}_t\|_0 \leq s$ **then**

$\mathbf{v}^{(t)} = \mathbf{x}_t / \|\mathbf{x}_t\|_2$

else

 Let A_t be the indices of the elements in \mathbf{x}_t with the largest s absolute values

$\mathbf{v}^{(t)} = \text{TRC}(\mathbf{x}_t, A_t) / \|\text{TRC}(\mathbf{x}_t, A_t)\|_2$

end if

$t \leftarrow t + 1$

until Convergence

References

- Amini, A. and Wainwright, M. (2009). High-dimensional analysis of semidefinite relaxations for sparse principal components. *The Annals of Statistics*, 37(5B):2877–2921.
- Berthet, Q. and Rigollet, P. (2013). Optimal detection of sparse principal components in high dimension. *The Annals of Statistics*, 41(4):1780–1815.
- Bickel, P. and Levina, E. (2008). Regularized estimation of large covariance matrices. *The Annals of Statistics*, 36(1):199–227.
- Birnbaum, A., Johnstone, I. M., Nadler, B., and Paul, D. (2013). Minimax bounds for sparse PCA with noisy high-dimensional data. *The Annals of Statistics*, 41(4):1055–1084.
- Bühlmann, P. and van de Geer, S. (2011). *Statistics for High-Dimensional Data: Methods, Theory and Applications*. Springer.
- Cai, T. T., Ma, Z., and Wu, Y. (2013). Sparse PCA: Optimal rates and adaptive estimation. *the Annals of Statistics (to appear)*.
- Choi, K. and Marden, J. (1998). A multivariate version of kendall’s τ . *Journal of Nonparametric Statistics*, 9(3):261–293.
- Croux, C., Ollila, E., and Oja, H. (2002). Sign and rank covariance matrices: statistical properties and application to principal components analysis. *Statistics for Industry and Technology*, pages 257–69.

- d'Aspremont, A., El Ghaoui, L., Jordan, M. I., and Lanckriet, G. R. (2007). A direct formulation for sparse PCA using semidefinite programming. *SIAM review*, 49(3):434–448.
- Di Martino, A., Yan, C., Li, Q., Denio, E., Castellanos, F., Alaerts, K., Anderson, J., Assaf, M., Bookheimer, S., Dapretto, M., et al. (2013). The autism brain imaging data exchange: towards a large-scale evaluation of the intrinsic brain architecture in autism. *Molecular Psychiatry (to appear)*.
- Eloyan, A., Muschelli, J., Nebel, M., Liu, H., Han, F., Zhao, T., Barber, A., Joel, S., Pekar, J., Mostofsky, S., et al. (2012). Automated diagnoses of attention deficit hyperactive disorder using magnetic resonance imaging. *Frontiers in Systems Neuroscience*, 6:61.
- Fang, K., Kotz, S., and Ng, K. (1990). Symmetric multivariate and related distributions. *Chapman&Hall, London*.
- Hallin, M., Oja, H., and Paindaveine, D. (2006). Semiparametrically efficient rank-based inference for shape. II. Optimal R-estimation of shape. *The Annals of Statistics*, 34(6):2757–2789.
- Hallin, M. and Paindaveine, D. (2002a). Optimal procedures based on interdirections and pseudo-Mahalanobis ranks for testing multivariate elliptic white noise against ARMA dependence. *Bernoulli*, 8(6):787–815.
- Hallin, M. and Paindaveine, D. (2002b). Optimal tests for multivariate location based on interdirections and pseudo-Mahalanobis ranks. *The Annals of Statistics*, 30(4):1103–1133.
- Hallin, M. and Paindaveine, D. (2004). Rank-based optimal tests of the adequacy of an elliptic VARMA model. *The Annals of Statistics*, 32(6):2642–2678.
- Hallin, M. and Paindaveine, D. (2005). Affine-invariant aligned rank tests for the multivariate general linear model with VARMA errors. *Journal of Multivariate Analysis*, 93(1):122–163.
- Hallin, M. and Paindaveine, D. (2006). Semiparametrically efficient rank-based inference for shape. I. Optimal rank-based tests for sphericity. *The Annals of Statistics*, 34(6):2707–2756.
- Han, F. and Liu, H. (2012). Semiparametric principal component analysis. In *Advances in Neural Information Processing Systems 25*, pages 171–179.
- Han, F. and Liu, H. (2013). Scale-invariant sparse PCA on high dimensional meta-elliptical data. *Journal of the American Statistical Association (to appear)*.

- Han, F., Zhao, T., and Liu, H. (2013). CODA: High dimensional copula discriminant analysis. *The Journal of Machine Learning Research*, 14:629–671.
- Hult, H. and Lindskog, F. (2002). Multivariate extremes, aggregation and dependence in elliptical distributions. *Advances in Applied Probability*, 34(3):587–608.
- Jackson, D. and Chen, Y. (2004). Robust principal component analysis and outlier detection with ecological data. *Environmetrics*, 15(2):129–139.
- Johnstone, I. and Lu, A. (2009). On consistency and sparsity for principal components analysis in high dimensions. *Journal of the American Statistical Association*, 104(486):682–693.
- Jolliffe, I., Trendafilov, N., and Uddin, M. (2003). A modified principal component technique based on the lasso. *Journal of Computational and Graphical Statistics*, 12(3):531–547.
- Journée, M., Nesterov, Y., Richtárik, P., and Sepulchre, R. (2010). Generalized power method for sparse principal component analysis. *The Journal of Machine Learning Research*, 11:517–553.
- Jung, S. and Marron, J. (2009). PCA consistency in high dimension, low sample size context. *The Annals of Statistics*, 37(6B):4104–4130.
- Kang, J. (2013). ABIDE data preprocessing. *personal communication*.
- Lindskog, F., McNeil, A., and Schmock, U. (2003). Kendall’s tau for elliptical distributions. *Credit Risk–Measurement, Evaluation and Management*, pages 149–156.
- Liu, H., Han, F., and Zhang, C.-H. (2012). Transelliptical graphical modeling under a hierarchical latent variable framework. *Technical Report*.
- Liu, L., Hawkins, D. M., Ghosh, S., and Young, S. S. (2003). Robust singular value decomposition analysis of microarray data. *Proceedings of the National Academy of Sciences*, 100(23):13167–13172.
- Lounici, K. (2013). Sparse principal component analysis with missing observations. *Progress in Probability*, 66:327–356.
- Ma, Z. (2013). Sparse principal component analysis and iterative thresholding. *The Annals of Statistics*, 41(2):772–801.
- Mackey, L. (2009). Deflation methods for sparse PCA. *Advances in Neural Information Processing Systems*, 21:1017–1024.

- Marden, J. (1999). Some robust estimates of principal components. *Statistics & Probability Letters*, 43(4):349–359.
- Meinshausen, N. and Bühlmann, P. (2006). High-dimensional graphs and variable selection with the lasso. *The Annals of Statistics*, 34(3):1436–1462.
- Neter, J., Kutner, M., Wasserman, W., and Nachtsheim, C. (1996). *Applied linear statistical models*, volume 4. Irwin Chicago.
- Oja, H. (2010). *Multivariate Nonparametric Methods with R: An Approach based on Spatial Signs and Ranks*, volume 199. Springer.
- Oja, H. and Paindaveine, D. (2005). Optimal signed-rank tests based on hyperplanes. *Journal of Statistical Planning and Inference*, 135(2):300–323.
- Oja, H. and Randles, R. H. (2004). Multivariate nonparametric tests. *Statistical Science*, 19(4):598–605.
- Oja, H., Sirkiä, S., and Eriksson, J. (2006). Scatter matrices and independent component analysis. *Austrian Journal of Statistics*, 35(2):175–189.
- Pavel, C. et al. (2005). *Statistical Tools for Finance and Insurance*. Springer.
- Posekany, A., Felsenstein, K., and Sykacek, P. (2011). Biological assessment of robust noise models in microarray data analysis. *Bioinformatics*, 27(6):807–814.
- Rachev, S. T. (2003). *Handbook of Heavy Tailed Distributions in Finance*, volume 1. Elsevier.
- Ruttimann, U. E., Unser, M., Rawlings, R. R., Rio, D., Ramsey, N. F., Mattay, V. S., Hommer, D. W., Frank, J. A., and Weinberger, D. R. (1998). Statistical analysis of functional MRI data in the wavelet domain. *IEEE Transactions on Medical Imaging*, 17(2):142–154.
- Shen, D., Shen, H., and Marron, J. (2011). Consistency of sparse PCA in high dimension, low sample size contexts. *arXiv preprint arXiv:1104.4289*.
- Shen, H. and Huang, J. (2008). Sparse principal component analysis via regularized low rank matrix approximation. *Journal of Multivariate Analysis*, 99(6):1015–1034.
- Sirkiä, S., Taskinen, S., and Oja, H. (2007). Symmetrised M-estimators of multivariate scatter. *Journal of Multivariate Analysis*, 98(8):1611–1629.
- Taskinen, S., Kankainen, A., and Oja, H. (2003). Sign test of independence between two random vectors. *Statistics & Probability Letters*, 62(1):9–21.

- Trefethen, L. N. and Bau III, D. (1997). *Numerical Linear Algebra*. Society for Industrial and Applied Mathematics.
- Tyler, D. E. (1982). Radial estimates and the test for sphericity. *Biometrika*, 69(2):429–436.
- Tyler, D. E. (1987). A distribution-free M -estimator of multivariate scatter. *The Annals of Statistics*, 15(1):234–251.
- Tzourio-Mazoyer, N., Landeau, B., Papathanassiou, D., Crivello, F., Etard, O., Delcroix, N., Mazoyer, B., and Joliot, M. (2002). Automated anatomical labeling of activations in SPM using a macroscopic anatomical parcellation of the MNI MRI single-subject brain. *Neuroimage*, 15(1):273–289.
- Vershynin, R. (2010). Introduction to the non-asymptotic analysis of random matrices. *arXiv preprint arXiv:1011.3027*.
- Visuri, S., Koivunen, V., and Oja, H. (2000). Sign and rank covariance matrices. *Journal of Statistical Planning and Inference*, 91(2):557–575.
- Vu, V. and Lei, J. (2012). Minimax rates of estimation for sparse PCA in high dimensions. *Proceedings of the 15th International Conference on Artificial Intelligence and Statistics (AISTATS)*, 22:1278–1286.
- Vu, V. Q. and Lei, J. (2013). Minimax sparse principal subspace estimation in high dimensions. *the Annals of Statistics (to appear)*.
- Witten, D., Tibshirani, R., and Hastie, T. (2009). A penalized matrix decomposition, with applications to sparse principal components and canonical correlation analysis. *Biostatistics*, 10(3):515–534.
- Yuan, X. and Zhang, T. (2013). Truncated power method for sparse eigenvalue problems. *The Journal of Machine Learning Research*, 14:899–925.
- Zhang, Y. and El Ghaoui, L. (2011). Large-scale sparse principal component analysis with application to text data. *Advances in Neural Information Processing Systems*.
- Zou, H., Hastie, T., and Tibshirani, R. (2006). Sparse principal component analysis. *Journal of Computational and Graphical Statistics*, 15(2):265–286.